

Tangential Fixpoint Iterations for Gromov–Wasserstein Barycenters

Florian Beier* and Robert Beinert*

Abstract. The Gromov–Wasserstein (GW) transport problem is a relaxation of classic optimal transport, which seeks a transport between two measures while preserving their internal geometry. Due to meeting this theoretical underpinning, it is a valuable tool for the analysis of objects that do not possess a natural embedding or should be studied independently of it. Prime applications can thus be found in e.g. shape matching, classification and interpolation tasks. To tackle the latter, one theoretically justified approach is the employment of multi-marginal GW transport and GW barycenters, which are Fréchet means with respect to the GW distance. However, because the computation of GW itself already poses a quadratic and non-convex optimization problem, the determination of GW barycenters is a hard task and algorithms for their computation are scarce. In this paper, we revisit a known procedure for the determination of Fréchet means in Riemannian manifolds via tangential approximations in the context of GW. We provide a characterization of barycenters in the GW tangent space, which ultimately gives rise to a fixpoint iteration for approximating GW barycenters using multi-marginal plans. We propose a relaxation of this fixpoint iteration and show that it monotonously decreases the barycenter loss. In certain cases our proposed method naturally provides us with barycentric embeddings. The resulting algorithm is capable of producing qualitative shape interpolations between multiple 3d shapes with support sizes of over thousands of points in reasonable time. In addition, we verify our method on shape classification and multi-graph matching tasks.

1. Introduction. Optimal transport (OT) focuses on transporting one given measure to another while minimizing some given cost. The interest of OT is twofold. Firstly, a solution to the problem, i.e. an optimal transport plan gives a means of correspondence between the input measures. Secondly, the value of the functional at a minimizer also gauges their divergence with respect to the underlying cost function. For a broad overview on the subject we refer to [46]. As its formulation is very general, OT has applications in a wide range of topics such as image matching [64, 66], signal processing [23] and particle dynamics [34, 33]. Moreover, due to relaxations and associated efficient approximate solvers, OT is now an established tool in machine learning [8, 27, 35]. The most prominent relaxation is entropy-regularized OT which can be solved by the parallelizable Sinkhorn algorithm [18]. Other efficient approximate solvers rely on e.g. slicing strategies [50, 48, 49], restriction to Gaussian mixture models [20] and low-rank restrictions [25, 54]. A generalization of OT which concerns itself with transporting between more than two input measures is multi-marginal OT [15]. The resulting formulation can be used to characterize OT barycenters which are Fréchet means with respect to the OT divergence [1]. Independently of barycenters, multi-marginal OT also finds applications in e.g. matching for teams [15], particle tracking [12], density functional theory [43]. The metric version of OT, namely the Wasserstein distance, has been a major focus in- and outside of the OT community. Here measures are considered to be members of the same underlying metric space and the associated cost function in the transport problem is a power of a metric. The Wasserstein space is then obtained by equipping the space of probability measures with finite

*Institute of Mathematics, Technische Universität Berlin, Straße des 17. Juni 136, 10623 Berlin, Germany (f.beier@tu-berlin.de, robert.beinert@tu-berlin.de).

moments with the Wasserstein distance. The Wasserstein space is a metric space and exhibits a rich Riemannian structure which has been extensively studied in [52, 6] and gives rise to the very active study of Wasserstein gradient flows [31, 2, 40, 29, 30, 6, 32, 42, 44, 7, 22].

A shortcoming of the Wasserstein distance is that it is heavily dependent on the embedding of the given input measures. One line of work, namely Gromov–Wasserstein (GW) transport, which has been sparked by Sturm [56] focuses on relaxations of OT to obtain an embedding-free comparison and matching of so-called metric measure (mm-) spaces. In addition to a measure, an mm-space possesses additional internal geometrical structure in the form of a metric. Sturms proposed transport problem is a twofold minimization over all measure-preserving isometric embeddings of either input into a common ambient metric space and over associated Wasserstein transport plans. The proposed transport problem has desirable properties such as independence of isometric transformations of either inputs. Although theoretically appealing, solving the proposed problem in practice is intractable. With the same idea in mind, Mémoli [38] proposed an alternative transport problem between mm-spaces which is now widely known as the GW distance. Although non-convex and quadratic, the problem is more accessible from a numerical standpoint. Because of this improved accessibility and since the GW distance meets the same theoretical underpinnings as Sturms construction, it is a valuable tool for matching and comparison tasks where inputs do not possess a natural embedding or should be studied independently of it. The proposed distance and transport problem thus has natural applications in e.g. shape matching [38], graph analysis [41], word alignment [4] and particle dynamics [9]. Solving GW still poses a non-convex, quadratic optimization problem, which motivated the OT community to propose several relaxations, most of which are inspired from the OT case. Examples are entropy-regularized GW [47, 65], low-rank constrained GW [55] and sliced GW [59, 13]. A fast exact solver for GW for inputs in low-dimensional Euclidean space has been presented in [51]. Recently, multi-marginal GW (MGW) has been proposed which exhibits similar connections to GW barycenters, i.e. Fréchet means with respect to the GW distance, as in the Wasserstein setting [11]. In [57], Sturm showed that using the GW distance, a metric space can be constructed which exhibits a similar Riemannian structure as the Wasserstein space. This additional structure can be leveraged e.g. for achieving a computational speedup when tasks require all pairwise distances of a large dataset. This potential has been explored in the Wasserstein case [64, 39] as well as in the GW case [10]. A fruitful iterative method for the approximation of Fréchet means or barycenters on Riemannian manifolds is as follows: lift the inputs into the tangent space at a reference point, determine the associated tangent barycenter and update the reference point by projecting back to the manifold [45]. This Fréchet mean method has been successfully used to obtain a simple fixpoint iteration to approximate Wasserstein barycenters and multi-marginal optimal transport [3, 63]. To the best of our knowledge, the only work which follows a similar idea in the GW case is [16]. However, in the reference, the authors assume the given spaces to be finite and then consider a gradient descent of the Fréchet functional. The nature of the provided proofs build strongly on the assumed discreteness and do not translate to the general case. Moreover, a characterization of Fréchet means in the GW tangent space is not given.

In this work, we are motivated by approximating GW barycenters via the previously mentioned Fréchet mean method. We study the tangent space and provide a characterization of tangential barycenters. The latter gives rise to a theoretically justified fixpoint iteration for

GW barycenter computation. We propose a relaxation of it which has desirable properties. Firstly, it can be easily implemented and only requires a solver for the GW transport problem. Secondly, we show that it monotonously decreases the GW barycenter functional. Furthermore, a single iteration of our proposed method is often sufficient to obtain a barycenter, e.g. when merely considering two inputs or any number of Gaussian spaces endowed with the standard scalar product. Existing state-of-the-art algorithms often have the undesirable property that computed approximate barycenters do not come with an embedding. Depending on the task, this may require numerically expensive embedding techniques. We discuss special cases, where our method naturally provides us with an embedding of the barycenter. We show an auxiliary result which states that there exists a GW barycenter between Gaussian spaces endowed with the standard scalar product which is again a Gaussian space. We run numerical experiments, showing that our method is capable of producing qualitative shape interpolations between multiple 3d shapes with support sizes of over 5000 points. To the best of our knowledge, no existing GW-based method is able to achieve this. Our experiments indicate that, in practice, running our method once produces the entire interpolation between the given inputs. In addition, we show that our method can be used to classify 3d shapes and to obtain multi-graph matchings.

Main Contributions.

- Justification of the Fréchet mean method for the GW case in [Theorem 5.3](#). More precisely, we show that the required barycenters in the GW tangent space always exist and can be characterized by multi-marginal plans.
- Relaxation of the Fréchet mean method in the form of a simple-to-implement fixpoint iteration. We show that this iteration decreases the barycenter loss monotonously, see [Theorem 6.2](#). Furthermore, [Theorem 6.3](#) shows that every subsequence of this fixpoint iteration contains a converging subsequence whose limit is an actual fixpoint. Notice that every GW barycenter is a fixpoint of the relaxed Fréchet mean procedure.
- For Gaussian distributions endowed with the Euclidean scalar product, we analytically characterize a GW barycenter as a Gaussian distribution with the same Euclidean scalar product, see [Theorem 5.2](#).

Our paper is organized as follows. [Section 2](#) provides the reader with the fundamental definitions and preliminary results related to GW transport. In [Section 3](#), we define the multi-marginal formulation of the GW problem. Following [\[57\]](#), [Section 4](#) discusses the Riemannian structure and gives the definition of the tangent space. In [Section 5](#) we introduce the GW barycenter problem and show its one-to-one correspondence to multi-marginal GW transport plans. We proceed with the definition of the tangential GW barycenter problem and characterize its solutions. In [Section 6](#), we propose a relaxed fixpoint iteration to approximate GW barycenters by a sequence of projected tangential barycenters. We show that the sequence monotonously decreases the GW barycenter loss. [Section 7](#) shows how the fixpoint iteration can be algorithmically implemented and discusses related practicalities. [Section 8](#) provides three numerical experiments indicating the potential of our proposed method.

2. Gauged Measure Spaces and Gromov–Wasserstein. For any Polish space X , we denote the related Borel σ -algebra by $\mathcal{B}(X)$, the set of signed Borel measures by $\mathcal{M}(X)$, the set of positive Borel measures by $\mathcal{M}^+(X)$, and the set of Borel probability measures by $\mathcal{P}(X)$.

If $\Phi: X \rightarrow Y$ is Borel measurable between the Polish spaces X and Y , the *push forward* of $\xi \in \mathcal{P}(X)$ by Φ is defined via

$$(\Phi_{\#}\xi)(A) := (\xi \circ \Phi^{-1})(A), \quad A \in \mathcal{B}(Y).$$

Depending on $\xi \in \mathcal{P}(X)$, any symmetric and square-integrable function $g: X \times X \rightarrow \mathbb{R}$ with respect to the product measure $\xi \otimes \xi$ is called a *gauge*. The *set of all gauges* on X with respect to ξ is denoted by $\mathfrak{G}(X, \xi) := L_{\text{sym}}^2(X \times X, \xi \otimes \xi)$. For every map $\Psi: Y \rightarrow X$, the *pull back* of g through Ψ is defined as

$$(\Psi^{\#}g)(y, y') := g(\Psi(y), \Psi(y')), \quad y, y' \in Y.$$

Any triple $\mathcal{X} := (X, g, \xi)$ consisting of

- a Polish space X ,
- a measure $\xi \in \mathcal{P}(X)$,
- a gauge $g \in \mathfrak{G}(X, \xi)$

is called a *gauged measure space (gm-space)*. Figuratively, the measure describes how the space is weighted whereas the gauge provides geometrical information. An important case of gm-spaces are obtained by choosing a metric as gauge. These spaces are also called metric measure spaces (mm-spaces). Popular other choices are (powers of) metrics, inner products, and adjacency matrices in the realm of graph matching.

The Gromov–Wasserstein (GW) distance between two gm-spaces $\mathcal{X} := (X, g, \xi)$ and $\mathcal{Y} := (Y, h, \nu)$ is an optimal-transport-based pseudometric. Henceforth, we denote the *set of transport plans* between \mathcal{X} and \mathcal{Y} by $\Pi(\mathcal{X}, \mathcal{Y}) := \{\pi \in \mathcal{P}(X \times Y) : (P_X)_{\#}\pi = \xi, (P_Y)_{\#}\pi = \nu\}$, where P_{\bullet} signifies the projection to the indicated component. The *GW-2* or just *GW distance* is given as

$$(2.1) \quad \text{GW}_2(\mathcal{X}, \mathcal{Y}) := \inf_{\pi \in \Pi(\mathcal{X}, \mathcal{Y})} F_{\text{GW}}^{\mathcal{X}, \mathcal{Y}}(\pi)$$

with the GW functional

$$(2.2) \quad \begin{aligned} F_{\text{GW}}^{\mathcal{X}, \mathcal{Y}}(\pi) &:= \|g(\cdot_1, \cdot_3) - h(\cdot_2, \cdot_4)\|_{L_{\text{sym}}^2(\pi(\cdot_1, \cdot_2) \otimes \pi(\cdot_3, \cdot_4))} \\ &:= \left(\iint_{(X \times Y)^2} |g(x, x') - h(y, y')|^2 d\pi(x, y) d\pi(x', y') \right)^{\frac{1}{2}}. \end{aligned}$$

The infimum in (2.1) is always attained [57, Prop 5.4], and we denote the *set of (GW-) optimal transport plans* by $\Pi_{\text{o}}(\mathcal{X}, \mathcal{Y})$. Two gm-spaces \mathcal{X} and \mathcal{Y} are called *homomorphic* ($\mathcal{X} \simeq \mathcal{Y}$) if $\text{GW}(\mathcal{X}, \mathcal{Y}) = 0$. In this case, there exist a third gm-space $\mathcal{Z} := (Z, f, \zeta)$ as well as Borel-measurable maps $\Phi: Z \rightarrow X$ and $\Psi: Z \rightarrow Y$ such that $\xi = \Phi_{\#}\zeta$, $\nu = \Psi_{\#}\zeta$, and $f = \Phi^{\#}g = \Psi^{\#}h$, see [57, Prop 5.6]. In particular, $\mathcal{X} \simeq \mathcal{Y}$ if there exists a map $\Phi: X \rightarrow Y$ such that $\nu = \Phi_{\#}\xi$ and $g = \Phi^{\#}h$. The homomorphic equivalence class of \mathcal{X} is denoted by $\mathfrak{X} := \llbracket \mathcal{X} \rrbracket$, and the *space of homomorphic gm-spaces* is expressed as \mathfrak{M} . The GW distance defines a metric on \mathfrak{M} . Moreover, $(\mathfrak{M}, \text{GW})$ is a complete, geodesic metric space, see [57, Thm 5.8].

Every gm-space $\mathbb{X} := (X, g, \xi)$ is a Lebesgue–Rokhlin space, which means that $\xi \in \mathcal{P}(X)$ can be characterized via the Lebesgue measure λ on the unit interval $[0, 1]$, cf. [57, Lem 1.15]. More precisely, there exists a Borel-measurable map $\Phi: [0, 1] \rightarrow X$ so that $\Phi_{\#}\lambda = \xi$. The map Φ may be chosen with respect to the atomic decomposition with finite or infinite many atoms:

$$\xi = \sum_{n=1}^{\infty} \xi_n \delta_{x_n} + \tilde{\xi},$$

where $\xi_n \in [0, 1]$ is the weight of the Dirac measure at $x_n \in X$, and $\tilde{\xi} \in \mathcal{M}^+(X)$ the remaining diffuse part. On the basis of the partition

$$(2.3) \quad I_n := [M_{n-1}, M_n) \quad \text{and} \quad I_{\infty} := [M_{\infty}, 1] \quad \text{with} \quad M_n := \sum_{m=1}^n \xi_m, \quad n \in \mathbb{N} \cup \{\infty\},$$

the *parametrization* Φ of \mathbb{X} can be chosen such that $\Phi(I_n) \equiv x_n$ and that the restriction $\Phi|_{I_{\infty}}: I_{\infty} \rightarrow \text{supp}(\tilde{\xi})$ is bijective with Borel-measurable inverse. The *set of parametrizations* of \mathbb{X} is expressed as $\mathfrak{P}(\mathbb{X})$ and is independent of the actual gauge. For any $\Phi \in \mathfrak{P}(\mathbb{X})$, \mathbb{X} is obviously homomorphic to $\mathbb{I} := ([0, 1], \bar{g}, \lambda)$ with $\bar{g} := \Phi^{\#}g$, which essentially allows us to restrict ourselves to gm-spaces over $[0, 1]$. The next result shows that the parametrization can be carried over to (optimal) transport plans between arbitrary gm-spaces.

Lemma 2.1. *Let the gm-spaces $\mathbb{X} := (X, g, \xi)$ and $\mathbb{Y} := (Y, h, \nu)$ be homomorphic to $\mathbb{I} := ([0, 1], \bar{g}, \lambda)$ and $\mathbb{J} := ([0, 1], \bar{h}, \lambda)$ via the parametrizations $\Phi \in \mathfrak{P}(\mathbb{X})$ and $\Psi \in \mathfrak{P}(\mathbb{Y})$ respectively. Then*

$$\Pi(\mathbb{X}, \mathbb{Y}) = (\Phi \times \Psi)_{\#}\Pi(\mathbb{I}, \mathbb{J}) \quad \text{and} \quad \Pi_{\circ}(\mathbb{X}, \mathbb{Y}) = (\Phi \times \Psi)_{\#}\Pi_{\circ}(\mathbb{I}, \mathbb{J}).$$

Proof. On the basis of the following atomic decompositions $\xi = \sum_{n=1}^{\infty} \xi_n \delta_{x_n} + \tilde{\xi}$ and $\nu = \sum_{m=1}^{\infty} \nu_m \delta_{y_m} + \tilde{\nu}$, any $\pi \in \Pi(\mathbb{X}, \mathbb{Y})$ admits the form

$$(2.4) \quad \pi = \sum_{n,m=1}^{\infty} \pi_{n,m} \delta_{(x_n, y_m)} + \tilde{\pi} \quad \text{with} \quad \tilde{\pi} = \sum_{n=1}^{\infty} \tilde{\pi}_{n,\infty} + \sum_{m=1}^{\infty} \tilde{\pi}_{\infty,m} + \tilde{\pi}_{\infty,\infty},$$

where the weight $\pi_{n,m}$ describes the partial transport from δ_{x_n} to δ_{y_m} , the measure $\tilde{\pi}_{n,\infty}$ the partial transport from δ_{x_n} to $\tilde{\nu}$, the measure $\tilde{\pi}_{\infty,m}$ the partial transport from $\tilde{\xi}$ to δ_{y_m} , and the measure $\tilde{\pi}_{\infty,\infty}$ the partial transport from $\tilde{\xi}$ to $\tilde{\nu}$. For the non-atomic parts $\tilde{\pi}_{\bullet,\bullet}$, the total masses are expressed by $\pi_{\bullet,\bullet} := \tilde{\pi}_{\bullet,\bullet}(X \times Y)$. Without loss of generality, let $\Phi \in \mathfrak{P}(\mathbb{X})$ and $\Psi \in \mathfrak{P}(\mathbb{Y})$ be chosen with respect to the atomic decomposition of ξ and ν as described in (2.3). Recall that Φ and Ψ are bijective with Borel-measurable inverse on $\text{supp}(\tilde{\xi})$ and $\text{supp}(\tilde{\nu})$. To distinguish the spaces $[0, 1]$ of \mathbb{I} and \mathbb{J} , we write $\mathbb{I} = (I, \bar{g}, \lambda)$ with partition $(I_n)_{n \in \mathbb{N} \cup \{\infty\}}$ and $\mathbb{J} = (J, \bar{h}, \lambda)$ with $(J_m)_{m \in \mathbb{N} \cup \{\infty\}}$. For any $\pi \in \Pi(\mathbb{X}, \mathbb{Y})$, we now define $\bar{\pi} \in \mathcal{P}(I \times J)$ via

$$\begin{aligned} \bar{\pi}|_{I_n \times J_m} &:= \frac{\pi_{n,m}}{\xi_n \nu_m} (\lambda|_{I_n} \otimes \lambda|_{J_m}), & \bar{\pi}|_{I_n \times J_{\infty}} &:= \frac{1}{\xi_n} (\lambda|_{I_n} \otimes \Psi_{\#}^{-1}(P_Y)_{\#}\tilde{\pi}_{n,\infty}), \\ \bar{\pi}|_{I_{\infty} \times J_m} &:= \frac{1}{\nu_m} (\Phi_{\#}^{-1}(P_X)_{\#}\tilde{\pi}_{\infty,m} \otimes \lambda|_{J_m}), & \bar{\pi}|_{I_{\infty} \times J_{\infty}} &:= (\Phi^{-1} \times \Psi^{-1})_{\#}\tilde{\pi}_{\infty,\infty}. \end{aligned}$$

The marginals of $\bar{\pi}$ are given by

$$(P_I)_{\#}\bar{\pi}|_{I_n} = \frac{1}{\xi_n} \left(\sum_{m=1}^{\infty} \pi_{n,m} + \pi_{n,\infty} \right) \lambda|_{I_n} = \lambda|_{I_n}, \quad n \in \mathbb{N},$$

$$(P_I)_{\#}\bar{\pi}|_{I_\infty} = \sum_{m=1}^{\infty} \Phi_{\#}^{-1}(P_X)_{\#}\tilde{\pi}_{\infty,m} + \Phi_{\#}^{-1}(P_X)_{\#}\tilde{\pi}_{\infty,\infty} = \Phi_{\#}^{-1}\tilde{\xi} = \lambda|_{I_\infty},$$

and analogously $(P_J)_{\#}\bar{\pi} = \lambda$, which shows $\bar{\pi} \in \Pi(\mathbb{I}, \mathbb{J})$. Computing $(\Phi \times \Psi)_{\#}\bar{\pi}|_{I_\bullet \times J_\bullet}$, we obtain all terms in (2.4) yielding $\Pi(\mathbb{X}, \mathbb{Y}) \subset (\Phi \times \Psi)_{\#}\Pi(\mathbb{I}, \mathbb{J})$. To show the opposite inclusion, we calculate the marginals of $(\Phi \times \Psi)_{\#}\bar{\pi}$ for any $\bar{\pi} \in \Pi(\mathbb{I}, \mathbb{J})$, which are

$$(P_X)_{\#}(\Phi \times \Psi)_{\#}\bar{\pi} = \Phi_{\#}(P_I)_{\#}\bar{\pi} = \Phi_{\#}\lambda = \xi$$

and similarly $(P_Y)_{\#}\pi = v$. Hence $(\Phi \times \Psi)_{\#}\Pi(\mathbb{I}, \mathbb{J}) = \Pi(\mathbb{X}, \mathbb{Y})$. Finally, for each pair $\pi \in \Pi(\mathbb{X}, \mathbb{Y})$ and $\bar{\pi} \in \Pi(\mathbb{I}, \mathbb{J})$ with $\pi = (\Phi, \Psi)_{\#}\bar{\pi}$, we have

$$F_{\text{GW}}^{\mathbb{X}, \mathbb{Y}}(\pi) = \|g(\cdot, \cdot, \cdot) - h(\cdot, \cdot, \cdot)\|_{L_{\text{sym}}^2(\pi \otimes \pi)} = \|\bar{g}(\cdot, \cdot, \cdot) - \bar{h}(\cdot, \cdot, \cdot)\|_{L_{\text{sym}}^2(\bar{\pi} \otimes \bar{\pi})} = F_{\text{GW}}^{\mathbb{I}, \mathbb{J}}(\bar{\pi}).$$

Since the GW distance is independent of the representative, meaning $\text{GW}(\mathbb{X}, \mathbb{Y}) = \text{GW}(\mathbb{I}, \mathbb{J})$, we thus have $\Pi_{\circ}(\mathbb{X}, \mathbb{Y}) = (\Phi \times \Psi)_{\#}\Pi_{\circ}(\mathbb{I}, \mathbb{J})$. \blacksquare

The GW distance between $\mathfrak{X} \in \mathfrak{M}$ and $\mathfrak{Y} \in \mathfrak{M}$ is, by construction, independent of the current representative, i.e. $\text{GW}(\mathfrak{X}, \mathfrak{Y}) := \text{GW}(\mathbb{X}, \mathbb{Y})$ for any $\mathbb{X} \in \mathfrak{X}$ and $\mathbb{Y} \in \mathfrak{Y}$. In order to transfer an (optimal) plan $\pi \in \Pi(\mathbb{X}, \mathbb{Y})$ between different representatives, we use gluings and meltings as an alternative to the parametrizations above. For the plans $\pi_1 \in \Pi(\mathbb{X}, \mathbb{Y})$ and $\pi_2 \in \Pi(\mathbb{X}, \mathbb{Z})$ between the gm-spaces $\mathbb{X} := (X, g, \xi)$, $\mathbb{Y} := (Y, h, v)$, and $\mathbb{Z} := (Z, f, \zeta)$, the *set of gluings* along \mathbb{X} is defined by

$$\Gamma_{\mathbb{X}}(\pi_1, \pi_2) := \Gamma_{\mathbb{X}}^{\mathbb{Y}, \mathbb{Z}}(\pi_1, \pi_2) := \{\gamma \in \mathcal{P}(X \times Y \times Z) : (P_{X \times Y})_{\#}\gamma = \pi_1, (P_{X \times Z})_{\#}\gamma = \pi_2\}.$$

Due to Dudley's lemma [5, Lem 8.4], the set of gluings is in particular non-empty. By construction, the 2-marginal $(P_{Y \times Z})_{\#}\gamma$ of any gluing $\gamma \in \Gamma_{\mathbb{X}}(\pi_1, \pi_2)$ lies in $\Pi(\mathbb{Y}, \mathbb{Z})$. This plan is also called a *melting* of π_1 and π_2 , cf. [57]. More generally, the *set of meltings* along \mathbb{X} is defined by

$$M_{\mathbb{X}}(\pi_1, \pi_2) := M_{\mathbb{X}}^{\mathbb{Y}, \mathbb{Z}}(\pi_1, \pi_2) := \{(P_{Y \times Z})_{\#}\gamma : \gamma \in \Gamma_{\mathbb{X}}(\pi_1, \pi_2)\}.$$

The sets of gluings and meltings can be extended to arbitrary $\Omega_1 \subset \Pi(\mathbb{X}, \mathbb{Y})$ and $\Omega_2 \subset \Pi(\mathbb{X}, \mathbb{Z})$ by setting

$$\Gamma_{\mathbb{X}}(\Omega_1, \Omega_2) := \bigcup_{\substack{\pi_1 \in \Omega_1 \\ \pi_2 \in \Omega_2}} \Gamma_{\mathbb{X}}(\pi_1, \pi_2) \quad \text{and} \quad M_{\mathbb{X}}(\Omega_1, \Omega_2) := \bigcup_{\substack{\pi_1 \in \Omega_1 \\ \pi_2 \in \Omega_2}} M_{\mathbb{X}}(\pi_1, \pi_2).$$

In the following, we will mainly use gluings and meltings to transfer (optimal) plans between different representatives.

Lemma 2.2. *Let \mathbb{X} , $\tilde{\mathbb{X}}$, and \mathbb{Y} be gm-spaces with $\mathbb{X} \simeq \tilde{\mathbb{X}}$. For any $\sigma \in \Pi_o(\mathbb{X}, \tilde{\mathbb{X}})$, it holds*

$$\Pi(\tilde{\mathbb{X}}, \mathbb{Y}) = M_{\mathbb{X}}(\sigma, \Pi(\mathbb{X}, \mathbb{Y})) \quad \text{and} \quad \Pi_o(\tilde{\mathbb{X}}, \mathbb{Y}) = M_{\mathbb{X}}(\sigma, \Pi_o(\mathbb{X}, \mathbb{Y})).$$

Proof. Let $\mathbb{X} := (X, g, \xi)$, $\tilde{\mathbb{X}} := (\tilde{X}, \tilde{g}, \tilde{\xi})$, and $\mathbb{Y} := (Y, h, \nu)$. As elaborated above, we obtain $M_{\mathbb{X}}(\sigma, \pi) \subset \Pi(\tilde{\mathbb{X}}, \mathbb{Y})$ for all $\pi \in \Pi(\mathbb{X}, \mathbb{Y})$, which ensures $M_{\mathbb{X}}(\sigma, \Pi(\mathbb{X}, \mathbb{Y})) \subset \Pi(\tilde{\mathbb{X}}, \mathbb{Y})$. The other way round, let $\tilde{\pi} \in \Pi(\tilde{\mathbb{X}}, \mathbb{Y})$ and $\gamma \in \Gamma_{\tilde{\mathbb{X}}}(\sigma^T, \tilde{\pi})$, where $\sigma^T \in \Pi_o(\tilde{\mathbb{X}}, \mathbb{X})$ denotes the reversion of $\sigma \in \Pi_o(\mathbb{X}, \tilde{\mathbb{X}})$. By construction, $\pi := (P_{X \times Y})_{\#} \gamma \in \Pi(\mathbb{X}, \mathbb{Y})$ and $(P_{X \times \tilde{X}})_{\#} \gamma = \sigma$. Hence, $\gamma \in \Gamma_{\mathbb{X}}(\sigma, \pi)$ and finally $\tilde{\pi} = (P_{\tilde{X} \times Y})_{\#} \gamma \in M_{\mathbb{X}}(\sigma, \pi)$. Thus, we obtain the first identity. For the second identity, let $\pi \in \Pi_o(\mathbb{X}, \mathbb{Y})$, we consider $\tilde{\pi} \in M_{\mathbb{X}}(\sigma, \pi)$ with underlying gluing $\gamma \in \Gamma_{\mathbb{X}}(\sigma, \pi)$. Since $g(\cdot_1, \cdot_3) = \tilde{g}(\cdot_2, \cdot_4)$ a.e. with respect to $\sigma(\cdot_1, \cdot_2) \otimes \sigma(\cdot_3, \cdot_4)$ and hence $g(P_X(\cdot_1), P_X(\cdot_3)) = \tilde{g}(P_{\tilde{X}}(\cdot_2), P_{\tilde{X}}(\cdot_4))$ a.e. with respect to $\gamma(\cdot_1, \cdot_2) \otimes \gamma(\cdot_3, \cdot_4)$, we have

$$\begin{aligned} \text{GW}(\mathbb{X}, \mathbb{Y}) &= F_{\text{GW}}^{\mathbb{X}, \mathbb{Y}}(\pi) = \iint_{(X \times \tilde{X} \times Y)^2} |g(x, x') - h(y, y')|^2 d\gamma(x, \tilde{x}, y) d\gamma(x', \tilde{x}', y') \\ &= \iint_{(X \times \tilde{X} \times Y)^2} |\tilde{g}(\tilde{x}, \tilde{x}') - h(y, y')|^2 d\gamma(x, \tilde{x}, y) d\gamma(x', \tilde{x}', y') = F_{\text{GW}}^{\tilde{\mathbb{X}}, \mathbb{Y}}(\tilde{\pi}) \geq \text{GW}(\tilde{\mathbb{X}}, \mathbb{Y}). \end{aligned}$$

Due to $\mathbb{X} \simeq \tilde{\mathbb{X}}$, the last inequality has to be tight showing $\tilde{\pi} \in \Pi_o(\tilde{\mathbb{X}}, \mathbb{Y})$. The opposite inclusion follows in an analogous way as in the first part. \blacksquare

If we melt a self-coupling $\sigma \in \Pi_o(\mathbb{X}, \mathbb{X})$ with an optimal plan $\pi \in \Pi_o(\mathbb{X}, \mathbb{Y})$, the resulting plans again lies in $\Pi_o(\mathbb{X}, \mathbb{Y})$. Every pair of plans that can be constructed in this manner are called equivalent, i.e. we say that $\pi_1, \pi_2 \in \Pi_o(\mathbb{X}, \mathbb{Y})$ are *equivalent* with respect to \mathbb{X} , written $\pi_1 \simeq_{\mathbb{X}} \pi_2$, if there exists $\sigma \in \Pi_o(\mathbb{X}, \mathbb{X})$ so that $\pi_1 \in M_{\mathbb{X}}(\sigma, \pi_2)$ and thus $\pi_2 \in M_{\mathbb{X}}(\sigma^T, \pi_1)$.

Proposition 2.3. *The relation $\simeq_{\mathbb{X}}$ is weakly continuous, i.e. if $\pi_2 \in \Pi_o(\mathbb{X}, \mathbb{Y})$ and $\pi_{1,n} \simeq_{\mathbb{X}} \pi_2$ for $n \in \mathbb{N}$ with $\pi_{1,n} \rightarrow \pi_1$, then $\pi_1 \simeq_{\mathbb{X}} \pi_2$.*

Proof. Without loss of generality, we consider the two copies $\mathbb{X}_1 := (I_1, \bar{g}, \lambda)$ and $\mathbb{X}_2 := (I_2, \bar{g}, \lambda)$ of \mathbb{X} , where $I_1 = I_2 = [0, 1]$. In the same way, let $\mathbb{Y} = (J, \bar{h}, \lambda)$ with $J = [0, 1]$. Since $\pi_{1,n} \simeq_{\mathbb{X}} \pi_2$, we have $\pi_{1,n} \in \Pi_o(\mathbb{X}_1, \mathbb{Y})$. Furthermore, due to [57, Lem. 5.5], it holds

$$F_{\text{GW}}^{\mathbb{X}_1, \mathbb{Y}}(\pi_1) = \lim_{n \rightarrow \infty} F_{\text{GW}}^{\mathbb{X}_1, \mathbb{Y}}(\pi_{1,n}) = \text{GW}(\mathbb{X}_1, \mathbb{Y}),$$

so that $\pi_1 \in \Pi_o(\mathbb{X}_1, \mathbb{Y})$. Let $\sigma_n \in \Pi_o(\mathbb{X}_1, \mathbb{X}_2)$ be so that $\pi_{1,n} \in M_{\mathbb{X}_2}(\sigma_n, \pi_2)$. We denote the corresponding gluing by $\gamma_n \in \Gamma_{\mathbb{X}_2}(\sigma_n, \pi_2)$, i.e. $(P_{I_1 \times J})_{\#} \gamma_n = \pi_{1,n}$. Since $(\gamma_n)_{n \in \mathbb{N}} \subset \Pi(\mathbb{X}_1, \mathbb{X}_2, \mathbb{Y})$ and the latter is weakly compact, we may extract a converging subsequence, i.e. $\gamma_{n_\ell} \rightarrow \gamma$ as $\ell \rightarrow \infty$. The marginal projections are weakly continuous, hence we obtain $(P_{I_1 \times J})_{\#} \gamma = \lim_{\ell \rightarrow \infty} \pi_{1,n_\ell} = \pi_1$ as well as $\sigma := (P_{I_1 \times I_2})_{\#} \gamma = \lim_{\ell \rightarrow \infty} \sigma_{n_\ell} \in \Pi_o(\mathbb{X}_1, \mathbb{X}_2)$. The optimality of σ can be shown analogously to the optimality of π_1 above. Finally, this gives $\gamma \in \Gamma_{\mathbb{Y}}(\sigma, \pi_1)$ with $(P_{I_2 \times J})_{\#} \gamma = \pi_2$ as desired. \blacksquare

3. Multi-Marginal GW. We focus on a multi-marginal formulation of (2.1), which has recently been proposed in [11]. To introduce the simultaneous transport between the gm-spaces $\mathbb{X}_i := (X_i, g_i, \xi_i)$ with $i = 1, \dots, N$, we denote the Cartesian product over the domains as $X_{\times} := \times_{i=1}^N X_i$ with elements $x_{\times} := (x_1, \dots, x_N)$, $x_i \in X_i$, and the *set of multi-marginal*

transport plans as $\Pi(\mathbb{X}_1, \dots, \mathbb{X}_N) := \{\pi \in \mathcal{P}(X_\times) : (P_{X_i})_\# \pi = \xi_i\}$. The $(N-1)$ -dimensional probability simplex is characterized by

$$\Delta_{N-1} := \{(\rho_1, \dots, \rho_N) \in [0, 1]^N : \sum_{i=1}^N \rho_i = 1\}.$$

For $\rho \in \Delta_{N-1}$, we define the *multi-marginal GW (MGW) problem* by

$$(3.1) \quad \text{MGW}_\rho(\mathbb{X}_1, \dots, \mathbb{X}_N) := \inf_{\pi \in \Pi(\mathbb{X}_1, \dots, \mathbb{X}_N)} F_{\text{MGW}_\rho}^{\mathbb{X}_1, \dots, \mathbb{X}_N}(\pi)$$

with the MGW functional

$$(3.2) \quad F_{\text{MGW}_\rho}^{\mathbb{X}_1, \dots, \mathbb{X}_N}(\pi) := \iint_{X_\times^2} \frac{1}{2} \sum_{i,j=1}^N \rho_i \rho_j |g_i(x_i, x'_i) - g_j(x_j, x'_j)|^2 d\pi(x_\times) d\pi(x'_\times).$$

The reason why we restrict ourselves to weights of the multiplicative form $\rho_i \rho_j$ in the respective summand will become evident when we introduce the free-support GW barycenter problem later on. Depending on the situation more general weights of the form $w_{i,j}$ may be considered. The *set of optimal plans* with respect to (3.1) is denoted by $\Pi_o^\rho(\mathbb{X}_1, \dots, \mathbb{X}_N)$, although we usually omit the superscript ρ if it is clear from context. The identities in [Lemma 2.1](#) generalize to the multi-marginal setting.

Lemma 3.1. *Let the gm-spaces $\mathbb{X}_i := (X_i, g_i, \xi_i)$ be homomorphic to $\mathbb{I}_i := ([0, 1], \bar{g}_i, \lambda)$ via the parametrization $\Phi_i \in \mathfrak{P}(\mathbb{X}_i)$ with $n = 1, \dots, N$. Then*

$$\Pi(\mathbb{X}_1, \dots, \mathbb{X}_N) = (\Phi_1 \times \dots \times \Phi_N)_\# \Pi(\mathbb{I}_1, \dots, \mathbb{I}_N)$$

and

$$\Pi_o(\mathbb{X}_1, \dots, \mathbb{X}_N) = (\Phi_1 \times \dots \times \Phi_N)_\# \Pi_o(\mathbb{I}_1, \dots, \mathbb{I}_N)$$

Proof. The first identity can be established using a similar construction as in the proof of [Lemma 2.1](#) by considering the transports between the different atomic and diffuse parts. The second identity follows from $F_{\text{MGW}_\rho}^{\mathbb{X}_1, \dots, \mathbb{X}_N}(\pi) = F_{\text{MGW}_\rho}^{\mathbb{I}_1, \dots, \mathbb{I}_N}(\bar{\pi})$ for every $\pi = (\Phi_1 \times \dots \times \Phi_N)_\# \bar{\pi}$. ■

An immediate consequence of the previous lemma is that the MGW problem is independent of the actual representation of the homomorphic classes—a property well known for the GW distance.

Proposition 3.2. *Let $\mathbb{X}_i \simeq \tilde{\mathbb{X}}_i$ for $i = 1, \dots, N$. Then*

$$\text{MGW}_\rho(\mathbb{X}_1, \dots, \mathbb{X}_N) = \text{MGW}_\rho(\tilde{\mathbb{X}}_1, \dots, \tilde{\mathbb{X}}_N).$$

In particular, $\text{MGW}_\rho(\mathfrak{X}_1, \dots, \mathfrak{X}_N) := \text{MGW}_\rho(\mathbb{X}_1, \dots, \mathbb{X}_N)$ with $\mathfrak{X}_i = [\mathbb{X}_i] \in \mathfrak{M}$ is well-defined.

Proof. The homomorphic equivalence of $\mathbb{X}_i = (X_i, g_i, \xi_i)$ and $\tilde{\mathbb{X}}_i = (\tilde{X}_i, \tilde{g}_i, \tilde{\xi}_i)$ ensures the existence of a third gm-space $\hat{\mathbb{X}}_i = (\hat{X}_i, \hat{g}_i, \hat{\xi}_i)$ and Borel-measurable maps $\Psi_i: \hat{X}_i \rightarrow X_i$ and $\tilde{\Psi}_i: \hat{X}_i \rightarrow \tilde{X}_i$ such that $\xi_i = (\Psi_i)_\# \hat{\xi}_i$, $\tilde{\xi}_i = (\tilde{\Psi}_i)_\# \hat{\xi}_i$, and $\hat{g}_i = \Psi_i^\# g_i = \tilde{\Psi}_i^\# \tilde{g}_i$. Any $\Theta_i \in \mathfrak{P}(\hat{\mathbb{X}}_i)$

induces the parametrizations $\Phi_i := \Psi_i \circ \Theta_i \in \mathfrak{P}(\mathbb{X}_i)$ and $\tilde{\Phi}_i := \tilde{\Psi}_i \circ \Theta_i \in \mathfrak{P}(\tilde{\mathbb{X}}_i)$ such that \mathbb{X}_i and $\tilde{\mathbb{X}}_i$ are homomorphic to $\mathbb{l}_i := ([0, 1], \bar{g}_i, \lambda)$ with $\bar{g}_i = \Phi_i^\# g_i = \tilde{\Phi}_i^\# \tilde{g}_i$. The assertion now follows from

$$F_{\text{MGW}_\rho}^{\mathbb{X}_1, \dots, \mathbb{X}_N}(\pi) = F_{\text{MGW}_\rho}^{\mathbb{l}_1, \dots, \mathbb{l}_N}(\bar{\pi}) = F_{\text{MGW}_\rho}^{\tilde{\mathbb{X}}_1, \dots, \tilde{\mathbb{X}}_N}(\tilde{\pi})$$

for $\pi = (\Phi_1 \times \dots \times \Phi_N) \# \bar{\pi}$ and $\tilde{\pi} = (\tilde{\Phi}_1 \times \dots \times \tilde{\Phi}_N) \# \bar{\pi}$ with $\bar{\pi} \in \Pi(\mathbb{l}_1, \dots, \mathbb{l}_N)$, and since [Lemma 3.1](#) further implies the equality of the infimum over all three MGW functionals. \blacksquare

Through the invariance of the MGW problem with respect to the homomorphic classes, the infimum over the MGW functional [\(3.2\)](#) is attained.

Theorem 3.3. *For the gm-spaces $\mathbb{X}_1, \dots, \mathbb{X}_N$, there exists a multi-marginal plan minimizing [\(3.2\)](#), i.e. $\Pi_o(\mathbb{X}_1, \dots, \mathbb{X}_N) \neq \emptyset$.*

Proof. Through [Lemma 3.1](#) and [Proposition 3.2](#), the claim is established by showing $\Pi_o(\mathbb{l}_1, \dots, \mathbb{l}_N) \neq \emptyset$, where $\mathbb{l}_i := (I_i, \bar{g}_i, \lambda)$, with $I_i := [0, 1]$, is homomorphic to $\mathbb{X}_i := (X_i, g_i, \xi_i)$ via some $\Phi_i \in \mathfrak{P}(\mathbb{X}_i)$. Let $(\bar{\pi}_k)_{k \in \mathbb{N}}$ with $\bar{\pi}_k \in \Pi(\mathbb{l}_1, \dots, \mathbb{l}_N)$ be a minimizing sequence of $F_{\text{MGW}_\rho}^{\mathbb{l}_1, \dots, \mathbb{l}_N}$ meaning $\lim_{k \rightarrow \infty} F_{\text{MGW}_\rho}^{\mathbb{l}_1, \dots, \mathbb{l}_N}(\bar{\pi}_k) = \text{MGW}(\mathbb{l}_1, \dots, \mathbb{l}_N)$. Since the measures $\bar{\pi}_k \in \mathcal{P}([0, 1]^N)$ defined on a compact support are tight, there exists a weakly convergence subsequence $(\bar{\pi}_{k_\ell})_{\ell \in \mathbb{N}}$. Furthermore, using the linearity of the integral and projecting the measure $\bar{\pi}_{k_\ell}$ onto the respective marginals, we obtain

$$\begin{aligned} & F_{\text{MGW}_\rho}^{\mathbb{l}_1, \dots, \mathbb{l}_N}(\bar{\pi}_{k_\ell}) \\ &= \frac{1}{2} \sum_{i,j=1}^N \rho_i \rho_j \iint_{(I_i \times I_j)^2} |g_i(x_i, x'_i) - g_j(x_j, x'_j)|^2 d(P_{I_i \times I_j}) \# \bar{\pi}_{k_\ell}(x_i, x_j) d(P_{I_i \times I_j}) \# \bar{\pi}_{k_\ell}(x'_i, x'_j). \end{aligned}$$

The integrals over the bi-marginal plans on the right-hand side are weakly continuous [[57](#), Lem 5.5]. Thus, $F_{\text{MGW}_\rho}^{\mathbb{l}_1, \dots, \mathbb{l}_N}$ is weakly continuous, and the weak limit of $(\bar{\pi}_{k_\ell})_{\ell \in \mathbb{N}}$ is a minimizer of [\(3.2\)](#). \blacksquare

4. GW Tangent Space. The space $(\mathfrak{M}, \text{GW})$ forms a Riemannian orbifold [[56](#)]. The reference contains an extensive study of the geometry of $(\mathfrak{M}, \text{GW})$, where the tangent space is constructed in the sense of Alexandrov by considering the completion of the set of geodesic directions with respect to a specific metric. Ultimately, the tangent space $\mathfrak{T}_\mathfrak{Y}$ at $\mathfrak{Y} \in \mathfrak{M}$ can be defined as the set of equivalence classes:

$$\mathfrak{T}_\mathfrak{Y} := \left(\bigcup_{(Y, h, v) \in \mathfrak{Y}} \mathfrak{G}(Y, v) \right) / \sim,$$

where the union is taken over all representatives (Y, h, v) of \mathfrak{Y} . Furthermore, $f \in \mathfrak{G}(Y, v)$ and $\tilde{f} \in \mathfrak{G}(\tilde{Y}, \tilde{v})$ related to the representatives $\mathfrak{Y} := (Y, h, v)$ and $\tilde{\mathfrak{Y}} := (\tilde{Y}, \tilde{h}, \tilde{v})$ are equivalent, i.e. $f \simeq \tilde{f}$, if there exists an optimal plan $\tau \in \Pi_o(\mathfrak{Y}, \tilde{\mathfrak{Y}})$ such that $f(\cdot_1, \cdot_3) = \tilde{f}(\cdot_2, \cdot_4)$ almost everywhere with respect to $\tau(\cdot_1, \cdot_2) \otimes \tau(\cdot_3, \cdot_4)$ on $(Y \times Y)^2$. Similarly to gm-spaces, the equivalence class of f is denoted by $\mathfrak{f} := \llbracket f \rrbracket$. Because any tangent representative $f \in \mathfrak{f}$ depends on the space representative $\mathfrak{Y} := (Y, h, v)$ on which it is defined, we introduce the notation $f|_\mathfrak{Y}$

whenever we want to emphasize this dependence. The space $\mathfrak{T}_{\mathfrak{Y}}$ becomes a complete metric space with the tangent metric:

$$(4.1) \quad d_{\mathfrak{T}_{\mathfrak{Y}}}(f, \tilde{f}) := \inf \{ \|f(\cdot_1, \cdot_3) - \tilde{f}(\cdot_2, \cdot_4)\|_{L^2_{\text{sym}}(\tau(\cdot_1, \cdot_2) \otimes \tau(\cdot_3, \cdot_4))} : \tau \in \Pi_o(\mathfrak{Y}, \tilde{\mathfrak{Y}}) \}$$

for any $f|_{\mathfrak{Y}} \in \mathfrak{f}$ and $\tilde{f}|_{\tilde{\mathfrak{Y}}} \in \tilde{\mathfrak{f}}$. Note that the tangent metric is independent of the chosen representatives. The infimum in (4.1) is always attained. Indeed, the objective can be written as $F_{\text{GW}}^{\mathbb{Z}, \tilde{\mathbb{Z}}}$ with $\mathbb{Z} = (Y, f, v)$, $\tilde{\mathbb{Z}} = (\tilde{Y}, \tilde{f}, \tilde{v})$. Leveraging a similar argument as in [Theorem 3.3](#), the minimizer can be constructed as a weak limit of elements in $\Pi_o(\mathfrak{Y}, \tilde{\mathfrak{Y}})$. Using [\[57, Lem. 5.5\]](#), we can show that this limit is element of $\Pi_o(\mathfrak{Y}, \tilde{\mathfrak{Y}})$ as well, cf. the proof of [Proposition 2.3](#).

The *exponential map* $\text{Exp}_{\mathfrak{Y}}: \mathfrak{T}_{\mathfrak{Y}} \rightarrow \mathfrak{M}$ is defined by

$$\text{Exp}_{\mathfrak{Y}}(f) := \llbracket (Y, h + f, v) \rrbracket \quad \text{for any } f|_{(Y, h, v)} \in \mathfrak{f}.$$

Conversely, the *logarithmic map* $\text{Log}_{\mathfrak{Y}}$ mapping \mathfrak{M} into a subset of $\mathfrak{T}_{\mathfrak{Y}}$ is given by

$$\text{Log}_{\mathfrak{Y}}(\mathfrak{X}) := \{ \llbracket (g - h)|_{(Y \times X, h, \pi)} \rrbracket : \mathfrak{Y} := (Y, h, v) \in \mathfrak{Y}, \mathfrak{X} := (X, g, \xi) \in \mathfrak{X}, \pi \in \Pi_o(\mathfrak{Y}, \mathfrak{X}) \}.$$

The transition from one representative to another representative in the definition of the logarithmic map can be described using optimal meltings.

Lemma 4.1. *Let $\mathfrak{X} := (X, g, \xi)$, $\mathfrak{Y} := (Y, h, v)$, and $\tilde{\mathfrak{Y}} := (\tilde{Y}, \tilde{h}, \tilde{v})$ be gm-spaces with $\mathfrak{Y} \simeq \tilde{\mathfrak{Y}}$. If $\pi \in \Pi(\mathfrak{Y}, \mathfrak{X})$ and $\sigma \in \Pi_o(\mathfrak{Y}, \tilde{\mathfrak{Y}})$, then*

$$(g - h)|_{(Y \times X, h, \pi)} \simeq (g - \tilde{h})|_{(\tilde{Y} \times X, \tilde{h}, \tilde{\pi})} \quad \text{for any } \tilde{\pi} \in M_{\mathfrak{Y}}(\sigma, \pi).$$

Proof. On the basis of the underlying gluing $\gamma \in \Gamma_{\mathfrak{Y}}(\sigma, \pi)$ of the chosen $\tilde{\pi} \in M_{\mathfrak{Y}}(\sigma, \pi)$, we consider $\tau := (P_Y, P_X, P_{\tilde{Y}}, P_X)_{\#} \gamma$. By the push-forward construction, τ is optimal in the sense of

$$\tau \in \Pi_o((Y \times X, h, \pi), (\tilde{Y} \times X, \tilde{h}, \tilde{\pi})).$$

Moreover, a short computation shows $(g - h)(\cdot_1, \cdot_3) = (g - \tilde{h})(\cdot_2, \cdot_4)$ almost everywhere with respect to $\tau(\cdot_1, \cdot_2) \otimes \tau(\cdot_3, \cdot_4)$ on $(Y \times X \times \tilde{Y} \times X)^2$ yielding the desired equivalence. \blacksquare

If $\pi \in \Pi_o(\mathfrak{Y}, \mathfrak{X})$, and thus $M_{\mathfrak{Y}}(\sigma, \pi) \subset \Pi_o(\tilde{\mathfrak{Y}}, \mathfrak{X})$ by [Lemma 2.2](#), then [Lemma 4.1](#) allows to switch between different representatives of \mathfrak{Y} in the definition of the logarithmic map. Similarly, we can transfer the logarithmic map between different representations of \mathfrak{X} .

5. Free-Support GW Barycenters. Barycenters are general Fréchet means on arbitrary metric spaces. For the GW setting, let $\mathfrak{X}_1, \dots, \mathfrak{X}_N$ be given gm-spaces, $\rho \in \Delta_{N-1}$ be given weights. An associated *GW barycenter* is any solution to

$$(5.1) \quad \text{GWB}_{\rho}(\mathfrak{X}_1, \dots, \mathfrak{X}_N) := \inf_{\mathfrak{Y} \in \mathfrak{M}} \mathcal{F}_{\text{GWB}_{\rho}}^{\mathfrak{X}_1, \dots, \mathfrak{X}_N}(\mathfrak{Y})$$

with the GW barycenter loss

$$(5.2) \quad \mathcal{F}_{\text{GWB}_{\rho}}^{\mathfrak{X}_1, \dots, \mathfrak{X}_N}(\mathfrak{Y}) := \sum_{i=1}^N \rho_i \text{GW}_2^2(\mathfrak{X}_i, \mathfrak{Y}).$$

Since the infimum in (5.1) is taken over arbitrary gm-spaces without restriction to their domain, the minimizer—whenever it exists—is called a *free-support GW barycenter*. The functional (5.2) is continuous with respect to the topology induced by the GW distance on \mathfrak{M} . For the special case of mm-spaces with compact support, there exists at least one barycenter, and every barycenter can be characterized as solution of an appropriate MGW problem [11, Thm 5.1]. This characterization carries over to the more general setting of gm-spaces, where the proof coincides line by line. For the sake of completeness, the detailed proof is given in [Appendix A](#).

Theorem 5.1. *Let $\mathfrak{X}_i := [(X_i, g_i, \xi_i)]$, $i = 1, \dots, N$, and $\rho \in \Delta_{N-1}$. There exists $\mathfrak{Y} \in \mathfrak{M}$ minimizing (5.1). Moreover, the homomorphic classes solving $\text{GWB}_\rho(\mathfrak{X}_1, \dots, \mathfrak{X}_N)$ are given by*

$$\left\{ \left[X_\times, \sum_{i=1}^N \rho_i g_i, \hat{\pi} \right] : \hat{\pi} \in \Pi_0^\rho(\mathfrak{X}_1, \dots, \mathfrak{X}_N) \right\}.$$

From a numerical perspective, the main issue of the free-support barycenter characterization in [Theorem 5.1](#) is the required optimal multi-marginal transport plan, whose computation for $N \geq 3$ is in general intractable. However, for Gaussian gm-spaces whose gauges are given by the standard scalar product, there exists a multi-marginal plan and GW barycenter with closed forms as the following result shows. The theorem makes use of the following notation: we denote the upper left $d \times d$ submatrix of any matrix B with $B^{(d)}$ and the diagonal sign matrices by

$$\mathcal{D}_d := \{\text{diag}(s_1, \dots, s_d) : s_k \in \{-1, 1\}\}.$$

The proof is provided in [Appendix B](#).

Theorem 5.2. *Let $d_1 \geq \dots \geq d_N \in \mathbb{N}$. Consider the gm-spaces $\mathfrak{X}_i = (\mathbb{R}^{d_i}, \langle \cdot, \cdot \rangle_{d_i}, \xi_i)$, where $\langle \cdot, \cdot \rangle_{d_i}$ is the standard scalar product on \mathbb{R}^{d_i} and $\xi_i = \mathcal{N}(0, \Sigma_i)$ are centered non-degenerate Gaussian distributions on \mathbb{R}^{d_i} , $i = 1, \dots, N$. Furthermore, let the covariance matrices Σ_i be diagonalized by $\Sigma_i = P_i D_i P_i^\top$ where the eigenvalues are sorted in decreasing order. For fixed $\tilde{I}_i \in \mathcal{D}_{d_i}$, let $T_i : \mathbb{R}^{d_1} \rightarrow \mathbb{R}^{d_i}$ be defined by*

$$(5.3) \quad T_i(x) = P_i A_i P_1^\top x, \quad A_i := \left(\tilde{I}_i D_i^{1/2} \left(D_1^{(d_i)} \right)^{-1/2} \Big| 0_{d_i, d_1 - d_i} \right) \in \mathbb{R}^{d_i \times d_1}.$$

For all $\rho \in \Delta_{N-1}$, it holds

$$(T_1, \dots, T_N) \# \xi_1 \in \Pi_0^\rho(\mathfrak{X}_1, \dots, \mathfrak{X}_N),$$

and

$$(5.4) \quad \mathfrak{Y} := (\mathbb{R}^{d_1}, \langle \cdot, \cdot \rangle_{d_1}, \hat{\nu}), \quad \hat{\nu} := \mathcal{N}\left(0, \sum_{i=1}^N \rho_i \underbrace{\begin{pmatrix} D_i & 0 \\ 0 & 0 \end{pmatrix}}_{\in \mathbb{R}^{d_1}}\right)$$

solves $\text{GWB}_\rho([\mathfrak{X}_1], \dots, [\mathfrak{X}_N])$.

The previous result generalizes both, [21, Prop 4.1] from the bi-marginal to the multi-marginal case, as well as [36, Thm. 3], which states that (5.4) is a solution to a restricted GW barycenter problem, where the gauge of the barycenter is a-priori fixed to be the inner product on Euclidean space.

As mentioned, in general the computation of optimal multi-marginal plans is intractable. For this reason, we adopt a known procedure to find Fréchet means on manifolds. The main idea is as follows: fix a reference point $\mathfrak{Y} \in \mathfrak{M}$ and lift $\mathfrak{X}_1, \dots, \mathfrak{X}_N$ into the tangent space $\mathfrak{T}_{\mathfrak{Y}}$ via the logarithmic map, determine a barycenter of the lifted gm-spaces in $\mathfrak{T}_{\mathfrak{Y}}$, project the barycenter back to \mathfrak{M} via the exponential map, and update \mathfrak{Y} . Iterate the procedure until convergence. In the following, we explore this tangential barycenter procedure in more detail. Selecting representatives $\mathbb{X}_i = (X_i, g_i, \xi_i) \in \mathfrak{X}_i$ and $\mathbb{Y} = (Y, h, v) \in \mathfrak{Y}$, fixing optimal plans $\pi_i \in \Pi_o(\mathbb{Y}, \mathbb{X}_i)$, and defining $\mathbb{Y}_i := (Y \times X_i, h, \pi_i)$, we consider the liftings

$$(5.5) \quad \mathfrak{g}_i := [(g_i - h)|_{\mathbb{Y}_i}] \in \mathbb{L}\text{og}_{\mathfrak{Y}}(\mathfrak{X}_i).$$

The *tangential barycenter* between $\mathfrak{g}_1, \dots, \mathfrak{g}_N$ with respect to barycentric coordinates $\rho \in \Delta_{N-1}$ is then the solution to

$$(5.6) \quad \text{GWTB}_{\rho}^{\mathfrak{Y}}(\mathfrak{g}_1, \dots, \mathfrak{g}_N) := \inf_{f \in \mathfrak{T}_{\mathfrak{Y}}} \mathcal{F}_{\text{GWTB}_{\rho}^{\mathfrak{Y}}}^{\mathfrak{g}_1, \dots, \mathfrak{g}_N}(f)$$

with the GW tangential barycenter loss

$$(5.7) \quad \mathcal{F}_{\text{GWTB}_{\rho}^{\mathfrak{Y}}}^{\mathfrak{g}_1, \dots, \mathfrak{g}_N}(f) := \sum_{i=1}^N \rho_i d_{\mathfrak{T}_{\mathfrak{Y}}}^2(\mathfrak{g}_i, f).$$

For the analysis of the tangential barycenter, we define the *set of (multi-marginal) gluings* between $\pi_i \in \Pi(\mathbb{Y}, \mathbb{X}_i)$ along \mathbb{Y} by

$$\Gamma_{\mathbb{Y}}(\pi_1, \dots, \pi_N) := \Gamma_{\mathbb{Y}}^{\mathbb{X}_1, \dots, \mathbb{X}_N}(\pi_1, \dots, \pi_N) := \{\gamma \in \mathcal{P}(Y \times X_{\times}) : (P_{Y \times X_i})_{\#} \gamma = \pi_i\}$$

and the *set of (multi-marginal) meltings* along \mathbb{Y} by

$$\text{M}_{\mathbb{Y}}(\pi_1, \dots, \pi_N) := \text{M}_{\mathbb{Y}}^{\mathbb{X}_1, \dots, \mathbb{X}_N}(\pi_1, \dots, \pi_N) := \{(P_{X_{\times}})_{\#} \gamma : \gamma \in \Gamma_{\mathbb{Y}}(\pi_1, \dots, \pi_N)\}.$$

Similarly as above, we extend these definitions to arbitrary sets of plans by taking the union of the elementwise gluings and meltings. For the sake of brevity, we rely on the following notation $\mathbb{Y}_{\times}[\gamma] := (Y \times X_{\times}, h, \gamma) \in \mathfrak{Y}$ for any $\gamma \in \mathcal{P}(Y \times X_{\times})$ with $(P_Y)_{\#} \gamma = v$ as well as on the mean gauge $m_{\rho}(x_{\times}, x'_{\times}) := \sum_{i=1}^N \rho_i g_i(x_i, x'_i)$ which is defined on X_{\times} .

Theorem 5.3. *The tangential barycenter problem (5.6) admits a solution. Moreover, there exist plans $\pi_i^* \simeq_{\mathbb{Y}} \pi_i$ so that $\mathfrak{m}_{\rho} := [(m_{\rho} - h)|_{\mathbb{Y}_{\times}(\gamma^*)}]$ is a tangential barycenter for some gluing $\gamma^* \in \Gamma_{\mathbb{Y}}(\pi_1^*, \dots, \pi_N^*)$.*

To prove the previous result, we require the following technical Lemma.

Lemma 5.4. *Let \mathfrak{g}_i be defined as in (5.5), and let $\mathfrak{f} \in \mathfrak{T}_{\mathfrak{Y}}$ be arbitrary. For every $f|_{\tilde{\mathfrak{Y}}} \in \mathfrak{f}$ defined on $\tilde{\mathfrak{Y}} := (\tilde{Y}, \tilde{h}, \tilde{\nu}) \in \mathfrak{Y}$, there exist $\tilde{\pi}_i \in \mathbb{M}_{\mathfrak{Y}}(\Pi_0(\mathfrak{Y}, \tilde{\mathfrak{Y}}), \pi_i)$ (dependent on f) so that*

$$\mathcal{F}_{\text{GWTB}_\rho^{\mathfrak{Y}}}^{\mathfrak{g}_1, \dots, \mathfrak{g}_N}(f) \geq \mathcal{F}_{\text{GWTB}_\rho^{\mathfrak{Y}}}^{\mathfrak{g}_1, \dots, \mathfrak{g}_N}(\tilde{\mathfrak{m}}) \quad \text{with} \quad \tilde{\mathfrak{m}}_\rho := \llbracket (m_\rho - \tilde{h})|_{\tilde{\mathfrak{Y}} \times [\tilde{\gamma}]} \rrbracket$$

for all gluings $\tilde{\gamma} \in \Gamma_{\tilde{\mathfrak{Y}}}(\tilde{\pi}_1, \dots, \tilde{\pi}_N)$ and $\tilde{\mathfrak{Y}}_\times[\tilde{\gamma}] := (\tilde{Y} \times X_\times, \tilde{h}, \tilde{\gamma})$.

Proof. Let $\tau_i \in \Pi_0(\tilde{\mathfrak{Y}}, \mathfrak{Y}_i)$ realize the tangent metric $d_{\mathfrak{T}_{\mathfrak{Y}}}^2(f|_{\tilde{\mathfrak{Y}}}, (g_i - h)|_{\mathfrak{Y}_i})$ in (4.1). Since $\sigma_i := (P_{Y \times \tilde{Y}})_\# \tau_i \in \Pi_0(\mathfrak{Y}, \tilde{\mathfrak{Y}})$, the marginal $\tilde{\pi}_i := (P_{\tilde{Y} \times X_i})_\# \tau_i \in \mathbb{M}_{\mathfrak{Y}}(\sigma_i, \pi_i)$ is optimal by Lemma 2.2. In analogy to above, we define $\tilde{\mathfrak{Y}}_i := (\tilde{Y} \times X_i, \tilde{h}, \tilde{\pi}_i)$. Using that $h(\cdot_1, \cdot_3) = \tilde{h}(\cdot_2, \cdot_4)$ a.e. with respect to each $\tau_i(\cdot_1, \cdot_2) \otimes \tau_i(\cdot_3, \cdot_4)$, we rewrite the tangential barycentric loss in (5.7) as

$$\begin{aligned} \mathcal{F}_{\text{GWTB}_\rho^{\mathfrak{Y}}}^{\mathfrak{g}_1, \dots, \mathfrak{g}_N}(f) &= \sum_{i=1}^N \rho_i \iint_{(\tilde{Y} \times Y \times X_i)^2} |f(\tilde{y}, \tilde{y}') - g_i(x_i, x'_i) + h(y, y')|^2 d\tau_i(\tilde{y}, y, x_i) d\tau_i(\tilde{y}', y', x'_i) \\ &= \sum_{i=1}^N \rho_i \iint_{(\tilde{Y} \times X_i)^2} |f(\tilde{y}, \tilde{y}') - g_i(x_i, x'_i) + \tilde{h}(\tilde{y}, \tilde{y}')|^2 d\tilde{\pi}_i(\tilde{y}, x_i) d\tilde{\pi}_i(\tilde{y}', x'_i) \\ &= \iint_{(\tilde{Y} \times X_\times)^2} \sum_{i=1}^N \rho_i |f(\tilde{y}, \tilde{y}') - g_i(x_i, x'_i) + \tilde{h}(\tilde{y}, \tilde{y}')|^2 d\tilde{\gamma}(\tilde{y}, x_\times) d\tilde{\gamma}(\tilde{y}', x'_\times), \end{aligned}$$

for an arbitrary gluing $\tilde{\gamma} \in \Gamma_{\tilde{\mathfrak{Y}}}(\tilde{\pi}_1, \dots, \tilde{\pi}_N)$. Exploiting that the functional $a \mapsto \sum_{i=1}^N \rho_i |a - a_i|^2$ is minimized by $a = \sum_{i=1}^N \rho_i a_i$ and applying this pointwisely inside the integral further yield

$$\begin{aligned} &\mathcal{F}_{\text{GWTB}_\rho^{\mathfrak{Y}}}^{\mathfrak{g}_1, \dots, \mathfrak{g}_N}(f) \\ &\geq \iint_{(\tilde{Y} \times X_\times)^2} \sum_{i=1}^N \rho_i |m_\rho(x_\times, x'_\times) - \tilde{h}(\tilde{y}, \tilde{y}') - g_i(x_i, x'_i) + \tilde{h}(\tilde{y}, \tilde{y}')|^2 d\tilde{\gamma}(\tilde{y}, x_\times) d\tilde{\gamma}(\tilde{y}', x'_\times) \end{aligned}$$

Writing $Z_\times := \tilde{Y} \times X_\times$ and $Z_i := \tilde{Y} \times X_i$, using $\tilde{\tau}_i := (P_{Z_\times}, P_{Z_i})_\# \tilde{\gamma} \in \Pi_0(\tilde{\mathfrak{Y}}_\times, \tilde{\mathfrak{Y}}_i)$, and taking the infimum over all optimal plans, we obtain

$$\begin{aligned} \mathcal{F}_{\text{GWTB}_\rho^{\mathfrak{Y}}}^{\mathfrak{g}_1, \dots, \mathfrak{g}_N}(f) &\geq \sum_{i=1}^N \rho_i \iint_{(Z_\times \times Z_i)^2} |(m_\rho - \tilde{h})(z_1, z'_1) - (g_i - \tilde{h})(z_2, z'_2)|^2 d\tilde{\tau}_i(z_1, z_2) d\tilde{\tau}_i(z'_1, z'_2) \\ &\geq \sum_{i=1}^N \rho_i d_{\mathfrak{T}_{\mathfrak{Y}}}^2((m_\rho - \tilde{h})|_{\tilde{\mathfrak{Y}}_\times[\tilde{\gamma}]}, (g_i - \tilde{h})|_{\tilde{\mathfrak{Y}}_i}) = \sum_{i=1}^N \rho_i d_{\mathfrak{T}_{\mathfrak{Y}}}^2((m_\rho - \tilde{h})|_{\tilde{\mathfrak{Y}}_\times[\tilde{\gamma}]}, (g_i - h)|_{\mathfrak{Y}_i}), \end{aligned}$$

where the last equality follows from Lemma 4.1 with σ_i from above. ■

Corollary 5.5. *Let \mathfrak{g}_i be defined as in (5.5), and let $\mathfrak{f} \in \mathfrak{T}_{\mathfrak{Y}}$ be arbitrary. Then there exist $\pi_i^* \simeq_{\mathfrak{Y}} \pi_i$ (dependent on \mathfrak{f}) so that*

$$\mathcal{F}_{\text{GWTB}_\rho^{\mathfrak{Y}}}^{\mathfrak{g}_1, \dots, \mathfrak{g}_N}(f) \geq \mathcal{F}_{\text{GWTB}_\rho^{\mathfrak{Y}}}^{\mathfrak{g}_1, \dots, \mathfrak{g}_N}(\mathfrak{m}_\rho) \quad \text{with} \quad \mathfrak{m} := \llbracket (m_\rho - h)|_{\mathfrak{Y}_\times[\gamma]} \rrbracket$$

for at least one gluing $\gamma \in \Gamma_{\mathfrak{Y}}(\pi_1^*, \dots, \pi_N^*)$.

Proof. Let $\tilde{\pi}_1, \dots, \tilde{\pi}_N$ be constructed as in the proof of Lemma 5.4 and consider a gluing $\tilde{\gamma} \in \Gamma_{\tilde{\mathbb{Y}}}(\tilde{\pi}_1, \dots, \tilde{\pi}_N)$. For fixed $\sigma \in \Pi_o(\tilde{\mathbb{Y}}, \mathbb{Y})$, Lemma 4.1 implies $(m_\rho - \tilde{h})|_{\tilde{\mathbb{Y}}_\times[\tilde{\gamma}]} \simeq (m_\rho - h)|_{\mathbb{Y}_\times[\gamma^*]}$ for $\gamma^* \in M_{\tilde{\mathbb{Y}}}(\sigma, \tilde{\gamma})$. Defining $\pi_i^* := (P_{Y \times X_i})_\# \gamma^*$, we readily obtain $\gamma^* \in \Gamma_{\mathbb{Y}}(\pi_1^*, \dots, \pi_N^*)$. The assertion $\pi_i^* \simeq_{\mathbb{Y}} \pi_i$ now follows from

$$\pi_i^* \in M_{\mathbb{Y}}(\sigma, \tilde{\pi}_i) \subset M_{\tilde{\mathbb{Y}}}(\sigma, M_{\mathbb{Y}}(\sigma_i, \pi_i)) = M_{\mathbb{Y}}(M_{\tilde{\mathbb{Y}}}(\sigma_i^T, \sigma), \pi_i)$$

since $M_{\tilde{\mathbb{Y}}}(\sigma_i^T, \sigma) \subset \Pi_o(\mathbb{Y}, \mathbb{Y})$ by Lemma 2.2. \blacksquare

The proof of Theorem 5.3 also requires the following continuity result, which is a multi-marginal variant of [57, Lem 5.5].

Lemma 5.6. *Let $I_\times := \times_{i=1}^M I_i$ be the unit cube with $I_i := [0, 1]$. For fixed $f_i \in \mathfrak{G}(I_i, \lambda)$, the mapping*

$$\Xi(\eta) := \left(\iint_{I_\times^2} \left| \sum_{i=1}^M f_i(x_i, x'_i) \right|^2 d\eta(x_1, \dots, x_M) d\eta(x'_1, \dots, x'_M) \right)^{\frac{1}{2}}$$

is continuous on $B_M := \{\eta \in \mathcal{P}(I_\times) : (P_{I_i})_\# \eta = \lambda\}$ equipped with the weak convergence from $\mathcal{P}(I_\times)$.

Proof. Similarly to the proof of [57, Lem 5.5], for every $\epsilon > 0$, there exists a symmetric, continuous function $f_{i,\epsilon} \in C_{\text{sym}}(I_i \times I_i)$ so that $\|f_i - f_{i,\epsilon}\|_{L^2_{\text{sym}}(\lambda \otimes \lambda)} \leq \epsilon$. For these functions, we analogously define $\Xi_\epsilon(\eta) := \|\sum_{i=1}^M f_{i,\epsilon}\|_{L^2_{\text{sym}}(\eta \otimes \eta)}$. Fixing $\eta \in B_M$, and using the triangle inequality twice, we have

$$|\Xi(\eta) - \Xi_\epsilon(\eta)| \leq \left\| \sum_{i=1}^M f_i - \sum_{i=1}^M f_{i,\epsilon} \right\|_{L^2_{\text{sym}}(\eta \otimes \eta)} \leq \sum_{i=1}^M \|f_i - f_{i,\epsilon}\|_{L^2_{\text{sym}}(\lambda \otimes \lambda)} \leq M\epsilon.$$

Let $\eta_n \rightharpoonup \eta$ be a weakly convergence sequence in B_M . Due to [11, Lem. A.1], we have $\eta_n \otimes \eta_n \rightharpoonup \eta \otimes \eta$ and thus $\Xi_\epsilon(\eta_n) \rightarrow \Xi_\epsilon(\eta)$. In total, we obtain

$$\lim_{n \rightarrow \infty} |\Xi(\eta_n) - \Xi(\eta)| \leq \lim_{n \rightarrow \infty} (|\Xi(\eta_n) - \Xi_\epsilon(\eta_n)| + |\Xi_\epsilon(\eta_n) - \Xi_\epsilon(\eta)| + |\Xi_\epsilon(\eta) - \Xi(\eta)|) \leq 2M\epsilon.$$

Since $\epsilon > 0$ is arbitrary, the continuity is established. \blacksquare

Proof of Theorem 5.3. Without loss of generality, we consider the representatives $\mathbb{X}_i := ([0, 1], g_i, \lambda)$, $\mathbb{Y} := ([0, 1], h, \lambda)$, and $\tilde{\mathbb{Y}} := ([0, 1], \tilde{h}, \lambda)$. Let $(\mathfrak{f}^{(n)})_{n \in \mathbb{N}} \subset \mathfrak{T}_{\mathfrak{g}}$ be a minimizing sequence of the tangent barycenter functional $\mathcal{F}_{\text{GWTB}_{\mathfrak{g}}^{\mathfrak{g}_1, \dots, \mathfrak{g}_N}}^{\mathfrak{g}_1, \dots, \mathfrak{g}_N}$ in (5.7). Due to Corollary 5.5, for every tangent $\mathfrak{f}^{(n)}$, there exists an $\mathfrak{m}_\rho^{(n)} := \llbracket (m_\rho - h)|_{\mathbb{Y}_\times[\gamma_n]} \rrbracket$ with $\gamma_n \in \Gamma_{\mathbb{Y}}(\pi_{1,n}^*, \dots, \pi_{N,n}^*)$, $\pi_{i,n}^* \simeq_{\mathbb{Y}} \pi_i$, such that

$$\mathcal{F}_{\text{GWTB}_{\mathfrak{g}}^{\mathfrak{g}_1, \dots, \mathfrak{g}_N}}^{\mathfrak{g}_1, \dots, \mathfrak{g}_N}(\mathfrak{f}^{(n)}) \geq \mathcal{F}_{\text{GWTB}_{\mathfrak{g}}^{\mathfrak{g}_1, \dots, \mathfrak{g}_N}}^{\mathfrak{g}_1, \dots, \mathfrak{g}_N}(\mathfrak{m}_\rho^{(n)});$$

so $(\mathfrak{m}_\rho^{(n)})_{n \in \mathbb{N}} \subset \mathfrak{T}_{\mathfrak{g}}$ is itself a minimizing sequence. Now let $\tau_{i,n} \in \Pi_o(\mathbb{Y}_i, \mathbb{Y}_\times[\gamma_n]) \subset \mathcal{P}([0, 1]^{N+3})$ realize $d_{\mathfrak{X}_{\mathfrak{g}}}^2(\mathfrak{g}_i, \mathfrak{m}_\rho^{(n)})$. Through the compact support, each sequence $(\tau_{i,n})_{n \in \mathbb{N}}$ is tight, and

we successively find subsequences such that $\tau_{i,n_\ell} \rightharpoonup \tau_i^*$ and $\gamma_{n_\ell} \rightharpoonup \gamma^*$, $\ell \rightarrow \infty$. Therefore $\tau_i^* \in \Pi(\mathbb{Y}_i, \mathbb{Y}_\times[\gamma^*])$. We denote the marginals $\pi_i^* := (P_{Y \times X_i})_\# \gamma^* = \lim_{n \rightarrow \infty} \pi_{i,n}^*$. Here, the last equality follows by the weak continuity of the marginal projections. Furthermore, due to the weak continuity of the relation $\simeq_{\mathbb{Y}}$, i.e. [Proposition 2.3](#), we obtain $\gamma^* \in \Gamma_{\mathbb{Y}}(\pi_1^*, \dots, \pi_N^*)$ with $\pi_i^* \simeq_{\mathbb{Y}} \pi_i$. Since the gauges of $\mathbb{Y}_\times[\gamma_n]$, $n \in \mathbb{N}$ and $\mathbb{Y}_\times[\gamma^*]$ coincide, [Lemma 5.6](#) moreover implies $\tau_i^* \in \Pi_o(\mathbb{Y}_i, \mathbb{Y}_\times[\gamma^*])$ with $\text{GW}(\mathbb{Y}_i, \mathbb{Y}_\times[\gamma^*]) = 0$. Making use of [Lemma 5.6](#) once again, we finally have

$$\begin{aligned} & \lim_{\ell \rightarrow \infty} \mathcal{F}_{\text{GWTB}_\rho^{\mathfrak{g}_1, \dots, \mathfrak{g}_N}}(\mathbf{m}_\rho^{(n_\ell)}) \\ &= \lim_{\ell \rightarrow \infty} \sum_{i=1}^N \rho_i \iint_{([0,1]^{N+3})^2} |(g_i - h)(\cdot_1, \cdot_3) - (m_\rho - h)(\cdot_2, \cdot_4)|^2 d\tau_{i,n}(\cdot_1, \cdot_2) d\tau_{i,n}(\cdot_3, \cdot_4) \\ &= \sum_{i=1}^N \rho_i \iint_{([0,1]^{N+3})^2} |(g_i - h)(\cdot_1, \cdot_3) - (m_\rho - h)(\cdot_2, \cdot_4)|^2 d\tau_i^*(\cdot_1, \cdot_2) d\tau_i^*(\cdot_3, \cdot_4) \\ &\geq \mathcal{F}_{\text{GWTB}_\rho^{\mathfrak{g}_1, \dots, \mathfrak{g}_N}}(\mathbf{m}_\rho^*) \quad \text{with} \quad \mathbf{m}_\rho^* := \llbracket (m_\rho - h)|_{\mathbb{Y}_\times[\gamma^*]} \rrbracket. \end{aligned}$$

Since $(\mathbf{m}_\rho^{(n_\ell)})_{\ell \in \mathbb{N}}$ is a minimizing sequence, \mathbf{m}_ρ^* has to be a minimizer and has the desired form. ■

[Theorem 5.3](#) motivates the following Fréchet mean procedure:

1. Choose representatives $\mathbb{X}_i \in \mathfrak{X}_i$.
2. Select a starting reference $\mathfrak{Y} := \llbracket \mathbb{Y} \rrbracket \in \mathfrak{M}$.
3. Compute $\pi_i \in \Pi_o(\mathbb{Y}, \mathbb{X}_i)$ to determine the liftings \mathfrak{g}_i in [\(5.5\)](#).
4. Find a tangential barycenter \mathbf{m}_ρ as in [Theorem 5.3](#).
5. Update $\mathfrak{Y} \leftarrow \text{Exp}_{\mathfrak{Y}}(\mathbf{m}_\rho)$, and repeat from step 3.

Note that the mean gauge of $\text{Exp}_{\mathfrak{Y}}(\mathbf{m}_\rho) = \llbracket (Y \times X_\times, m_\rho, \gamma^*) \rrbracket$ only depends on the subspace X_\times so that $\text{Exp}_{\mathfrak{Y}}(\mathbf{m}_\rho) = \llbracket (X_\times, m_\rho, (P_{X_\times})_\# \gamma^*) \rrbracket$. At its heart, this barycenter procedure is a fixpoint iteration of the set-valued mapping

$$\text{TB}_\rho(\mathfrak{Y}) := \{ \llbracket (X_\times, m_\rho, (P_{X_\times})_\# \gamma^*) \rrbracket : \gamma^* \in \Gamma_{\mathbb{Y}}(\pi_1^*, \dots, \pi_N^*) \text{ as in } \text{Theorem 5.3}, \mathbb{Y} \in \mathfrak{Y} \},$$

i.e. we consider the iteration $\mathfrak{Y}_{n+1} \in \text{TB}_\rho(\mathfrak{Y}_n)$ beginning from some $\mathfrak{Y}_0 \in \mathfrak{M}$.

6. Tangential Fixpoint Iteration. Unfortunately, the proposed tangential barycenter procedure is intractable in practice. In particular, the search for the minimizer \mathbf{m}_ρ in [Theorem 5.3](#) is unmanageable due to the lack of efficient methods to determine the gluing γ^* numerically. As a remedy, we relax the fixpoint iteration regarding TB_ρ and refrain from the exact minimization on $\mathfrak{T}_{\mathfrak{Y}}$. More precisely, we study the relaxed, set-valued mapping

$$\widetilde{\text{TB}}_\rho(\mathfrak{Y}) := \{ \llbracket (X_\times, m_\rho, \mu) \rrbracket : \mu \in \text{M}_{\mathfrak{Y}}^o(\mathbb{X}_1, \dots, \mathbb{X}_N) \}$$

with the *set of optimal meltings*

$$\text{M}_{\mathfrak{Y}}^o(\mathbb{X}_1, \dots, \mathbb{X}_N) := \{ \mu \in \text{M}_{\mathbb{Y}}(\pi_1, \dots, \pi_N) : \pi_i \in \Pi_o(\mathbb{Y}, \mathbb{X}_i) \}.$$

for any $\mathbb{Y} \in \mathfrak{Y}$. Note that $\text{M}_{\mathfrak{Y}}^o$ is independent of the chosen representative.

Proposition 6.1. *The mapping $\widetilde{\text{TB}}_\rho$ (as well as TB_ρ) is well-defined and independent from the selected representatives $\mathbb{X}_1, \dots, \mathbb{X}_N, \mathbb{Y}$.*

Proof. Initially, let the representatives $\mathbb{X}_i := (X_i, g_i, \xi_i) \in \mathfrak{X}$ be fixed and homomorphic to $\mathbb{I}_i = ([0, 1], \bar{g}_i, \lambda)$ via $\Phi_i \in \mathfrak{P}(\mathbb{X}_i)$. Similarly to the proof of [Proposition 3.2](#), for two representatives $\mathbb{Y} := (Y, h, v), \tilde{\mathbb{Y}} := (\tilde{Y}, \tilde{h}, \tilde{v}) \in \mathfrak{Y}$, we find parametrizations $\Psi \in \mathfrak{P}(\mathbb{Y})$ and $\tilde{\Psi} \in \mathfrak{P}(\tilde{\mathbb{Y}})$ so that \mathbb{Y} and $\tilde{\mathbb{Y}}$ are homomorphic to a common $\mathbb{J} = ([0, 1], \bar{h}, \lambda)$ via Ψ and $\tilde{\Psi}$. On account of [Lemma 2.1](#), for each $\pi_i \in \Pi_o(\mathbb{Y}, \mathbb{X}_i)$, there exists at least one $\bar{\pi}_i \in \Pi_o(\mathbb{J}, \mathbb{I}_i)$ such that $\pi_i = (\Psi \times \Phi_i)_\# \bar{\pi}_i$ and $\tilde{\pi}_i := (\tilde{\Psi} \times \Phi_i)_\# \bar{\pi}_i \in \Pi_o(\tilde{\mathbb{Y}}, \mathbb{X}_i)$. In analogy to [Lemma 3.1](#), for these plans, we have

$$\begin{aligned} \Gamma_{\mathbb{Y}}(\pi_1, \dots, \pi_N) &= (\Psi \times \Phi_1 \times \dots \times \Phi_N)_\# \Gamma_{\mathbb{J}}(\bar{\pi}_1, \dots, \bar{\pi}_N), \\ \Gamma_{\tilde{\mathbb{Y}}}(\tilde{\pi}_1, \dots, \tilde{\pi}_N) &= (\tilde{\Psi} \times \Phi_1 \times \dots \times \Phi_N)_\# \Gamma_{\mathbb{J}}(\bar{\pi}_1, \dots, \bar{\pi}_N). \end{aligned}$$

Determining the marginals with respect to X_\times and I_\times , we thus deduce

$$M_{\mathbb{Y}}(\pi_1, \dots, \pi_N) = (\Phi_1 \times \dots \times \Phi_N)_\# M_{\mathbb{J}}(\bar{\pi}_1, \dots, \bar{\pi}_N) = M_{\tilde{\mathbb{Y}}}(\tilde{\pi}_1, \dots, \tilde{\pi}_N).$$

Taking the union over all optimal plans, which are induced by $\Pi_o(\mathbb{J}, \mathbb{I}_i)$, we obtain the independence of $M_{\mathbb{Y}}^o$ from the actual representative $\mathbb{Y} \in \mathfrak{Y}$. A similar argument for the representatives of \mathfrak{X}_i yields that $\widetilde{\text{TB}}_\rho$ generates the same homomorphic classes for any $\mathbb{X}_i \in \mathfrak{X}$. \blacksquare

Different from the tangential barycenter procedure in the previous section, the elements of $\widetilde{\text{TB}}_\rho(\mathfrak{Y})$ are simply based on the N optimal GW plans and their melting. For this reason, the fixpoint iteration $\mathfrak{Y}_{n+1} \in \widetilde{\text{TB}}_\rho(\mathfrak{Y}_n)$ becomes numerically tractable. Despite the relaxation, this iteration yields a sequence with non-increasing barycentric loss, which can be seen as an analogue to the Wasserstein case in [\[3, Prop. 3.3\]](#).

Theorem 6.2. *Let $\mathfrak{X}_1, \dots, \mathfrak{X}_N, \mathfrak{Y} \in \mathfrak{OM}$ and $\rho \in \Delta_{N-1}$ be fixed. Then every $\mathfrak{Z} \in \widetilde{\text{TB}}_\rho(\mathfrak{Y})$ satisfies*

$$\mathcal{F}_{\text{GWB}_\rho}^{\mathfrak{X}_1, \dots, \mathfrak{X}_N}(\mathfrak{Y}) \geq \mathcal{F}_{\text{GWB}_\rho}^{\mathfrak{X}_1, \dots, \mathfrak{X}_N}(\mathfrak{Z}) + \text{GW}_2^2(\mathfrak{Y}, \mathfrak{Z}).$$

In particular, every barycenter \mathfrak{Y} is a fixpoint of $\widetilde{\text{TB}}_\rho$, i.e. $\mathfrak{Z} = \mathfrak{Y}$.

Remarkably, the previous result holds for all $\mathfrak{Z} \in \widetilde{\text{TB}}_\rho(\mathfrak{Y})$ where only the gauge of \mathfrak{Z} depends on ρ . Hence, for any arbitray fixed $\mu \in M_{\mathfrak{Y}}^o(\mathfrak{X}_1, \dots, \mathfrak{X}_N)$ and $\mathfrak{Z} = \llbracket (X_\times, m_\rho, \mu) \rrbracket$, the above inequality holds for all $\rho \in \Delta_{N-1}$.

Proof. We consider the representatives $\mathbb{X}_i := (X_i, g_i, \xi_i) \in \mathfrak{X}_i$ and $\mathbb{Y} := (Y, h, v) \in \mathfrak{Y}$. Since $\mathfrak{Z} \in \widetilde{\text{TB}}_\rho(\mathfrak{Y})$, there exist $\pi_i \in \Pi_o(\mathbb{Y}, \mathbb{X}_i)$ and $\gamma \in \Gamma_{\mathbb{Y}}(\pi_1, \dots, \pi_N)$ such that $\mathfrak{Z} := (X_\times, m_\rho, \mu) \in \mathfrak{Z}$ with $m_\rho := \sum_{i=1}^N g_i$ and $\mu := (P_{X_\times})_\# \gamma$. The barycentric loss of \mathfrak{Y} may be written as

$$\begin{aligned} \mathcal{F}_{\text{GWB}_\rho}^{\mathfrak{X}_1, \dots, \mathfrak{X}_N}(\mathfrak{Y}) &= \sum_{i=1}^N \rho_i \iint_{(Y \times X_i)^2} |h(y, y') - g_i(x_i, x'_i)|^2 d\pi_i(y, x_i) d\pi_i(y', x'_i) \\ &= \iint_{(Y \times X^\times)^2} \sum_{i=1}^N \rho_i |h(y, y') - g_i(x_i, x'_i)|^2 d\gamma(y, x_\times) d\gamma(y', x'_\times). \end{aligned}$$

Due to $\sum_{i=1}^N \rho_i |b - a_i|^2 = |b - a|^2 + \sum_{i=1}^N \rho_i |a - a_i|^2$ for $a := \sum_{i=1}^N \rho_i a_i$, we obtain

$$\begin{aligned} \mathcal{F}_{\text{GWB}_\rho}^{\mathfrak{X}_1, \dots, \mathfrak{X}_N}(\mathfrak{Y}) &= \iint_{(Y \times X \times X)^2} |h(y, y') - m_\rho(x_\times, x'_\times)|^2 d\gamma(y, x_\times) d\gamma(y', x'_\times) \\ &\quad + \sum_{i=1}^N \rho_i \iint_{X_\times^2} |m_\rho(x_\times, x'_\times) - g_i(x_i, x'_i)|^2 d\mu(x_\times) d\mu(x'_\times). \end{aligned}$$

We estimate the terms on the right-hand side separately. Since $\gamma \in \Pi(\mathbb{Y}, \mathbb{Z})$, it clearly holds

$$\iint_{(Y \times X \times X)^2} |h(y, y') - m_\rho(x_\times, x'_\times)|^2 d\gamma(y, x_\times) d\gamma(y', x'_\times) \geq \text{GW}_2^2(\mathbb{Y}, \mathbb{Z}) = \text{GW}_2^2(\mathfrak{Y}, \mathfrak{Z}).$$

Defining $\tilde{\pi}_i := (\text{Id}, P_{X_i})_{\#} \mu \in \Pi(\mathbb{Z}, \mathbb{X}_i)$, we further estimate the second term by

$$\begin{aligned} &\sum_{i=1}^N \rho_i \iint_{X_\times^2} |m_\rho(x_\times, x'_\times) - g_i(x_i, x'_i)|^2 d\mu(x_\times) d\mu(x'_\times) \\ &= \sum_{i=1}^N \rho_i \iint_{(X_\times \times X_i)^2} |m_\rho(x_\times, x'_\times) - g_i(\tilde{x}_i, \tilde{x}'_i)|^2 d\tilde{\pi}_i(x_\times, \tilde{x}_i) d\tilde{\pi}_i(x'_\times, \tilde{x}'_i) \\ &\geq \sum_{i=1}^N \rho_i \text{GW}_2^2(\mathbb{Z}, \mathbb{X}_i) = \sum_{i=1}^N \rho_i \text{GW}_2^2(\mathfrak{Z}, \mathfrak{X}_i) = \mathcal{F}_{\text{GWB}_\rho}^{\mathfrak{X}_1, \dots, \mathfrak{X}_N}(\mathfrak{Z}), \end{aligned}$$

which establishes the assertion. ■

Furthermore, every sequence iteratively generated by applying $\widetilde{\text{TB}}_\rho$ contains a convergent subsequence, whose limit can be interpreted as fixpoint of TB_ρ .

Theorem 6.3. *Let $\mathfrak{X}_1, \dots, \mathfrak{X}_N \in \mathfrak{M}$ and $\rho \in \Delta_{N-1}$ be fixed. Then every subsequence of $(\mathfrak{Y}_n)_{n \in \mathbb{N}}$ with $\mathfrak{Y}_{n+1} \in \text{TB}_\rho(\mathfrak{Y}_n)$ contains a convergent subsequence $\mathfrak{Y}_{n_\ell} \rightarrow \mathfrak{Y} \in \mathfrak{M}$ so that $\mathfrak{Y} \in \text{TB}_\rho(\mathfrak{Y})$.*

To give the proof, we require the following two lemmata about the continuity and stability of the GW transport on the box. For this, let $I_\times := \times_{i=1}^M I_i$ be the unit cube with $I_i := [0, 1]$, and consider the measures with uniform marginals given by $\text{B}_M := \{\eta \in \mathcal{P}(I_\times) : (P_{I_i})_{\#} \eta = \lambda\}$. We equip B_M with the weak convergence from $\mathcal{P}(I_\times)$.

Lemma 6.4. *For fixed $h_i \in \mathfrak{G}(I_i, \lambda)$, consider $\mathfrak{Y}_n := \llbracket (I_\times, h, v_n) \rrbracket$ with $h := \sum_{i=1}^M h_i$ and $v_n \in \text{B}_M$. If $v_n \rightarrow v \in \text{B}_M$, then $\mathfrak{Y}_n \rightarrow \mathfrak{Y} := \llbracket (I_\times, h, v) \rrbracket \in \mathfrak{M}$ as $n \rightarrow \infty$.*

Proof. Consider the representatives $\mathbb{Y}_n := (I_\times, h, v_n)$ and $\mathbb{Y} := (I_\times, h, v)$. As a direct consequence of [62, Thm. 5.20], for every subsequence of $(\mathbb{Y}_n)_{n \in \mathbb{N}}$, we can find a further subsequence $(\mathbb{Y}_{n_\ell})_{\ell \in \mathbb{N}}$ and plans $\pi_{n_\ell} \in \Pi(\mathbb{Y}_{n_\ell}, \mathbb{Y})$ such that $\pi_{n_\ell} \rightarrow \pi := (\text{Id}, \text{Id})_{\#} v$. [The plans can be constructed by considering the Wasserstein distance on $\mathcal{P}(I_\times)$.] Since the gauges of \mathbb{Y}_{n_ℓ} and \mathbb{Y} coincide, both GW functionals $F_{\text{GW}}^{\mathbb{Y}_{n_\ell}, \mathbb{Y}}$ and $F_{\text{GW}}^{\mathbb{Y}, \mathbb{Y}}$ become $\Xi(\bullet) := \|h(\cdot, \cdot) - h(\cdot, \cdot)\|_{L^2_{\text{sym}}(\bullet \otimes \bullet)}$. As $\pi_{n_\ell} \in \text{B}_{2M}$, Lemma 5.6 implies

$$\text{GW}(\mathbb{Y}_{n_\ell}, \mathbb{Y}) \leq \Xi(\pi_{n_\ell}) \rightarrow \Xi(\pi) = 0 \quad \text{as } \ell \rightarrow \infty.$$

Since this holds true for all subsequences, we obtain the assertion as desired. \blacksquare

To distinguish the different boxes, we define $I_{1,\times} := \times_{i=1}^{M_1} I_i$ and $I_{2,\times} := \times_{i=1}^{M_2} I_i$ with $I_i := [0, 1]$.

Lemma 6.5. *Consider $\mathbb{Y}_n := (I_{1,\times}, h, v_n)$ with $h := \sum_{i=1}^{M_1} h_i$, $h_i \in \mathfrak{G}(I_i, \lambda)$, and $v_n \in \mathbb{B}_{M_1}$, and let $\mathbb{X} = (I_{2,\times}, g, \xi)$ be given with $g := \sum_{i=1}^{M_2} g_i$, $g_i \in \mathfrak{G}(I_i, \lambda)$, and $\xi \in \mathbb{B}_{M_2}$. Furthermore, let $\pi_n \in \Pi_o(\mathbb{Y}_n, \mathbb{X})$, and assume $\pi_n \rightarrow \pi \in \mathbb{B}_{M_1+M_2}$. Then π is optimal between $\mathbb{Y} := (I_{1,\times}, h, v)$ with $v := (P_{I_{1,\times}})_{\#}\pi$ and \mathbb{X} , i.e. $\pi \in \Pi_o(\mathbb{Y}, \mathbb{X})$.*

Proof. Defining $\Xi(\eta) := \|h - g\|_{L^2_{\text{sym}}(\eta \otimes \eta)}$ for all $\eta \in \mathbb{B}_{M_1+M_2}$, we notice that Ξ coincides with the GW functional $F_{\text{GW}}^{\mathbb{Y}_n, \mathbb{X}}$ on $\Pi(\mathbb{Y}_n, \mathbb{X}) \subset \mathbb{B}_{M_1+M_2}$ and with $F_{\text{GW}}^{\mathbb{Y}, \mathbb{X}}$ on $\Pi(\mathbb{Y}, \mathbb{X}) \subset \mathbb{B}_{M_1+M_2}$. Hence, we have

$$(6.1) \quad |F_{\text{GW}}^{\mathbb{Y}, \mathbb{X}}(\pi) - \text{GW}(\mathbb{Y}, \mathbb{X})| \leq |\Xi(\pi) - \Xi(\pi_n)| + |\Xi(\pi_n) - \text{GW}(\mathbb{Y}, \mathbb{X})|.$$

By [Lemma 5.6](#), the first term converges to zero. Furthermore, the weak convergence of π_n implies $v_n \rightarrow v$, which yields $\llbracket \mathbb{Y}_n \rrbracket \rightarrow \llbracket \mathbb{Y} \rrbracket \in \mathfrak{M}$ due to [Lemma 6.4](#). Since π_n is optimal, we have $\Xi(\pi_n) = \text{GW}(\mathbb{Y}_n, \mathbb{X})$; so the second term in (6.1) converges to zero by the continuity of the metric. This shows $F_{\text{GW}}^{\mathbb{Y}, \mathbb{X}}(\pi) = \text{GW}(\mathbb{Y}, \mathbb{X})$ and thus $\pi \in \Pi_o(\mathbb{Y}, \mathbb{X})$ as desired. \blacksquare

Proof of Theorem 6.3. Without loss of generality, we consider the representatives $\mathbb{X}_i := (I_i, g_i, \lambda)$, where $I_i := [0, 1]$. As before, the related box is denoted by $I_{\times} := \times_{i=1}^N I_i$, and the mean gauge as $m_{\rho}(x_{\times}, x'_{\times}) := \sum_{i=1}^N \rho_i g_i(x_i, x'_i)$. Except for the starting space \mathfrak{Y}_1 , the elements of $(\mathfrak{Y}_n)_{n \in \mathbb{N}}$ are defined as $\mathfrak{Y}_n = \llbracket \mathbb{Y}_n \rrbracket$ with $\mathbb{Y}_n := (I_{\times}, m_{\rho}, \mu_n)$ for some melting $\mu_n \in \text{M}_{\mathfrak{Y}_{n-1}}(\mathbb{X}_1, \dots, \mathbb{X}_N) \subset \mathcal{P}(I_{\times})$. Let γ_n , $n \in \mathbb{N}$, be the associated gluings. For $n > 2$, we have $\gamma_n \in \mathcal{P}(I_{\times} \times I_{\times})$ with first marginal μ_{n-1} and second marginal μ_n . Since $I_{\times} \times I_{\times}$ is compact, the sequence γ_n is tight, and any subsequence contains a weakly convergent subsequence $\gamma_{n_{\ell}}$ with some limit $\gamma \in \mathcal{P}(I_{\times} \times I_{\times})$. Due to [Lemma 6.4](#), we have $\mathfrak{Y}_{n_{\ell}} \rightarrow \tilde{\mathfrak{Y}} := \llbracket \tilde{\mathbb{Y}} \rrbracket$ with $\tilde{\mathbb{Y}} := (I_{\times}, m, \tilde{\mu})$, where $\tilde{\mu}$ is the second marginal of γ , and $\mathfrak{Y}_{n_{\ell}-1} \rightarrow \mathfrak{Y} := \llbracket \mathbb{Y} \rrbracket$ with $\mathbb{Y} := (I_{\times}, m, \mu)$, where μ denotes the first marginal of γ . Since $(P_{I_{\times} \times I_i})_{\#}\gamma_{n_{\ell}} \in \Pi_o(\mathbb{Y}_{n_{\ell}-1}, \mathbb{X}_i)$, [Lemma 6.5](#) ensures the optimality of $(P_{I_{\times} \times I_i})_{\#}\gamma \in \Pi_o(\mathbb{Y}, \mathbb{X}_i)$; so we have $\tilde{\mu} \in \text{M}_{\mathfrak{Y}}(\mathbb{X}_1, \dots, \mathbb{X}_N)$ and $\tilde{\mathfrak{Y}} \in \widetilde{\text{TB}}_{\rho}(\mathfrak{Y})$. Furthermore, [Theorem 6.2](#) yields

$$\mathcal{F}_{\text{GWB}_{\rho}}^{\tilde{x}_1, \dots, \tilde{x}_N}(\mathfrak{Y}_{n_{\ell}-1}) \geq \mathcal{F}_{\text{GWB}_{\rho}}^{\tilde{x}_1, \dots, \tilde{x}_N}(\mathfrak{Y}_{n_{\ell}}) + \text{GW}_2^2(\mathfrak{Y}_{n_{\ell}-1}, \mathfrak{Y}_{n_{\ell}}).$$

Taking the limit over ℓ , and exploiting that $(\mathcal{F}_{\text{GWB}_{\rho}}(\mathfrak{Y}_n))_{n \in \mathbb{N}}$ is monotonically decreasing and bounded from below, we obtain $\text{GW}(\mathfrak{Y}, \tilde{\mathfrak{Y}}) = 0$, establishing the assertion. \blacksquare

7. Algorithm and Practical Usage.

7.1. Explicit Implementation of the Tangential Barycenter Method. The numerical fixpoint iteration with respect to $\widetilde{\text{TB}}_{\rho}$ is summarized in [Algorithm 7.1](#). Comments on the GW step and on the gluing-melting step can be found below. Choosing for instance $\mathbb{Y} = \mathbb{X}_1$ as the initial gm-space slightly reduces the computation of the algorithm in the first iteration since we may simply set $\hat{\pi}_1 := (\text{Id}, \text{Id})_{\#}\xi_1$ instead of computing the plan. Moreover, if we are in the case $N = 2$, for any computed $\hat{\pi}_2 \in \Pi_o(\mathbb{Y}, \mathbb{X}_2)$ it holds

$$\Gamma_{\mathbb{Y}}((\text{Id}, \text{Id})_{\#}\xi_1, \hat{\pi}_2) = \{(P_Y, P_Y, P_{X_2})_{\#}\pi_2\}, \quad \text{which yields} \quad \text{M}_{\mathbb{X}_1}((\text{Id}, \text{Id})_{\#}\xi_1, \hat{\pi}_2) = \{\hat{\pi}_2\}.$$

Algorithm 7.1 Tangential Barycenter Algorithm

Input: gm-spaces $\mathbb{X}_i := (X_i, g_i, \xi_i)$, $i = 1, \dots, N$,
barycentric coordinates $\rho \in \Delta_{N-1}$,
initial gm-space $\mathbb{Y} := (Y, h, \nu)$

while not converged **do**
GW Step: Compute optimal GW plans $\hat{\pi}_i$ between \mathbb{Y} and \mathbb{X}_i , $i = 1, \dots, N$.
Gluing-Melting Step: Construct a gluing $\gamma \in \Gamma_{\mathbb{Y}}(\hat{\pi}_1, \dots, \hat{\pi}_N)$ with melting $\mu := P_{X_{\times} \# \gamma}$.
Set $\mathbb{Y} \leftarrow (X_{\times}, \sum_{i=1}^N \rho_i g_i, \mu)$.

end while

Output: Approximate barycenter $\mathbb{Y} = (X_{\times}, \sum_{i=1}^N \rho_i g_i, \mu)$

Thus, after the first iteration \mathbb{Y} has the form

$$\mathbb{Y} = (X_1 \times X_2, \rho_1 g_1 + \rho_2 g_2, \hat{\pi}_2),$$

which is already a solution to $\text{GWB}_{(\rho_1, \rho_2)}(\mathbb{X}_1, \mathbb{X}_2)$, cf. [Theorem 5.1](#). In other words, [Algorithm 7.1](#) reaches optimality already after one iteration. The same holds true for N gm-spaces given as centered Gaussian distributions endowed with the standard Euclidean scalar product. Indeed, consider the setting from [Theorem 5.2](#), i.e. let $d_1 \geq \dots \geq d_N$ and $\mathbb{X}_i = (\mathbb{R}^{d_i}, \langle \cdot, \cdot \rangle_{d_i}, \xi_i)$, with $\xi_i = \mathcal{N}(0, \Sigma_i)$. Taking $\mathbb{Y} = \mathbb{X}_1$, we may set $\hat{\pi}_i = (\text{Id}, T_i)_{\#} \xi_1 \in \Pi_o(\mathbb{X}_1, \mathbb{X}_i)$ in the GW step, where T_i is defined as in [Theorem 5.2](#). This yields

$$\Gamma_{\mathbb{Y}}(\pi_1, \dots, \pi_N) = \{(\text{Id}, T_1, \dots, T_N)_{\#} \xi_1\} \quad \text{so that} \quad M_{\mathbb{Y}}(\pi_1, \dots, \pi_N) = \{(T_1, \dots, T_N)_{\#} \xi_1\}.$$

Due to [Theorem 5.2](#) we have $(T_1, \dots, T_N)_{\#} \xi_1 \in \Pi_o^{\rho}(\mathbb{X}_1, \dots, \mathbb{X}_N)$, so that optimality is reached after one iteration.

In the following, we provide some further insight on the practical application of [Algorithm 7.1](#), discuss the recovery of embeddings of the barycenters and show how an approximation of pairwise distances of the input spaces can be obtained.

The GW Step. At the heart of the iterations in [Algorithm 7.1](#) are the GW computations between $\mathbb{Y} = (Y, h, \nu)$ and $\mathbb{X}_i = (X_i, g_i, \xi_i)$, hence we comment on existing methods to compute GW which we use in our numerical section below. For a bigger picture, see e.g. [\[47, 65\]](#). One way to numerically approximate solutions of $\text{GW}(\mathbb{Y}, \mathbb{X}_i)$ is by performing a block-coordinate descent of the bi-convex relaxed problem

$$(7.1) \quad \inf_{\pi, \gamma \in \Pi(\nu, \xi_i)} \|h(\cdot_1, \cdot_3) - g_i(\cdot_2, \cdot_4)\|_{L_{\text{sym}}^2(\pi(\cdot_1, \cdot_2) \otimes \gamma(\cdot_3, \cdot_4))}^2.$$

Fixing, say, γ and minimizing with respect to π , we recover the Kantorovich problem

$$(7.2) \quad \inf_{\pi \in \Pi(\nu, \xi_i)} \int_{Y \times X_i} \|h(y, \cdot_3) - g_i(x, \cdot_4)\|_{L_{\text{sym}}^2(\gamma(\cdot_3, \cdot_4))}^2 d\pi(y, x).$$

Most practical algorithms for GW rely on this structure, i.e. for a fixed initial guess $\gamma \in \Pi(\nu, \xi_i)$ solve [\(7.2\)](#), then set $\gamma = \pi$ and repeat this iteration until a convergence criterion is

satisfied. The local problem may be solved directly, e.g. with the network simplex algorithm. Another option is to regularize (7.2) by adding an entropic regularizer like $+\varepsilon \text{KL}(\pi, \nu \otimes \xi_i)$, or $+\varepsilon \text{KL}(\pi, \gamma)$ to the functional, where KL denotes the Kullback–Leibler divergence. In both cases, this allows to leverage the Sinkhorn algorithm [18] for solving the local problem at the cost of the usual entropic blurring.

The Gluing-Melting Step. Let $\mathbb{Y} := (Y, h, \nu)$, $\mathbb{X}_i := (X_i, g_i, \xi_i)$ be gm-spaces with support sizes $m, n_i \in \mathbb{N}$, $i = 1, \dots, N$. Solutions that are obtained in the above way without regularization are naturally very sparse. More precisely, there exists a solution $\pi_i \in \Pi(\nu, \xi_i)$ to (7.2) with

$$|\text{supp}(\pi_i)| \leq m + n_i - 1 \ll n_i m,$$

see e.g. [26, Thm. 1]. In an effort to obtain a sparse gluing and keep computational complexity low, we propose to use the *north-west corner rule*, see e.g. [46, Sec. 3.4.2] for details. This generates a gluing $\gamma \in \Gamma_{\mathbb{Y}}(\pi_1, \dots, \pi_N)$ in up to $m + \sum_{i=1}^N n_i$ operations and ensures $|\text{supp}(\gamma)| \leq m + (\sum_{i=1}^N n_i) - N$. Using this construction, after k iterations of Algorithm 7.1, the support size of \mathbb{Y} can be bounded by

$$m + k \left(\sum_{i=1}^N n_i \right) - kN.$$

In contrast, for any approximate solution π_i of the regularized version of (7.2), it holds $|\text{supp}(\pi_i)| = n_i m$, $i = 1, \dots, N$. In this case $|\text{supp}(\gamma)| = m \prod_{i=1}^N n_i$ and thus $|\text{supp}(\mu)| = \prod_{i=1}^N n_i$ for any gluing $\gamma \in \Gamma_{\mathbb{Y}}(\pi_1, \dots, \pi_N)$ and associated melting $\mu \in \text{M}_{\mathbb{Y}}(\pi_1, \dots, \pi_N)$ which practically inhibits the use entropic regularizers. However, if additionally $|X_i| = m$ and ξ_i is the uniform distribution on X_i , $i = 1, \dots, N$, we propose the following alternative construction for the gluing-melting step. First, we initialize Algorithm 7.1 with $\mathbb{Y} = (Y, h, \nu)$ such that $|Y| = m$. After solving the GW step with entropic regularization to obtain measures $\pi_i \in \Pi(\mathbb{Y}, \mathbb{X}_i)$, we do the following. Iterating over $\ell = 1, \dots, m$, we recursively construct

$$T_i(x_\ell^{(i)}) = \operatorname{argmax} \left\{ \frac{\pi_i(\{(y, x_\ell^i)\})}{\nu(\{y\})} : y \in Y, T_i(x_{\tilde{\ell}}^{(i)}) \neq y, \tilde{\ell} = 1, \dots, \ell - 1 \right\}, \quad i = 1, \dots, N.$$

By construction, the obtained maps $T_i : X_i \rightarrow Y$ are invertible, so we may replace the gluing-melting step by instead setting

$$\tilde{\gamma} = (\text{Id}, T_1^{-1}, \dots, T_N^{-1})_{\#} \nu \quad \text{and} \quad \tilde{\mu} = P_{X_{\times}} \# \tilde{\gamma}.$$

Note that $\tilde{\gamma}$ and $\tilde{\mu}$ does not have to be an actual gluing and melting, respectively. The construction ensures $|\text{supp}(\tilde{\mu})| = m$ so that we may readily apply this procedure again in the next iteration. Figuratively, the multi-marginal plan $\tilde{\mu}$ inscribes one-to-one correspondences between the inputs by associating their points, if most of their respective masses is transported to the same point in \mathbb{Y} . In our practical application we refer to this procedure as the *maximum rule without replacement*. Since ξ_i is the uniform distribution on m points for all $i = 1, \dots, N$, we obtain $\tilde{\mu} \in \Pi(\mathbb{X}_1, \dots, \mathbb{X}_N)$. The maximum rule without replacement is particularly well suited when we are interested in exact one-to-one correspondences of the given inputs.

7.2. Embeddings for Barycenters. For certain practical tasks, an embedding of the GW interpolants may be required. However, finding an appropriate embedding can be a very challenging task on its own and is a common drawback for existing methods such as the state-of-the-art algorithm provided by Peyré, Cuturi and Solomon [47]. Here, the output of the function takes the form of a dissimilarity matrix which is usually embedded using some numerically expensive distance-preserving embedding technique like multi-dimensional scaling. A remedy to this has been proposed in [11], where the support of the sought barycenter is fixed a-priori. In the following, we want to give some insights on this embedding-issue in relation to our proposed method and give some special cases where (high-dimensional) embeddings of tangent barycenters can be obtained naturally. To this end, consider the inputs $\mathcal{X}_i = (X_i, g_i, \xi_i)$, $i = 1, \dots, N$, and let (X_\times, m_ρ, μ) with $\mu \in \Pi(\mathcal{X}_1, \dots, \mathcal{X}_N)$ be (an approximation of) the barycenter.

Euclidean Space. First, we consider the Euclidean case, i.e. let $X_i = \mathbb{R}^{d_i}$, $d_i \in \mathbb{N}$, $i = 1, \dots, N$, and set $d_\oplus := \sum_{i=1}^N d_i$.

i) Let $g_i := \|\cdot - \cdot\|_{d_i,1}$ be the 1-norm on \mathbb{R}^{d_i} , $i = 1, \dots, N$. Then

$$\begin{aligned} m_\rho(x_\times, x'_\times) &= \sum_{i=1}^N \rho_i g_i(x_i, x'_i) = \sum_{i=1}^N \rho_i \|x_i - x'_i\|_{d_i,1} = \sum_{i=1}^N \|\rho_i x_i - \rho_i x'_i\|_{d_i,1} \\ &= \|S_\rho(x_\times) - S_\rho(x'_\times)\|_{d_\oplus,1}, \end{aligned}$$

where $S_\rho(x_\times) := (\rho_1 x_1, \dots, \rho_N x_N)$, $x_\times \in X_\times$. Thus,

$$(X_\times, m_\rho, \mu) \simeq (\mathbb{R}^{d_\oplus}, \|\cdot - \cdot\|_{d_\oplus,1}, (S_\rho)_\# \mu).$$

ii) Either let $g_i = \|\cdot - \cdot\|_{d_i,2}^2$ be the squared standard Euclidean norm on \mathbb{R}^{d_i} or $g_i = \langle \cdot, \cdot \rangle_{d_i}$ be the standard scalar product on \mathbb{R}^{d_i} . Then we obtain

$$\begin{aligned} m_\rho(x_\times, x'_\times) &= \sum_{i=1}^N \rho_i g_i(x_i, x'_i) = \sum_{i=1}^N g_i(\sqrt{\rho_i} x_i, \sqrt{\rho_i} x'_i) \\ &= \begin{cases} \|S_{\sqrt{\rho}}(x_\times) - S_{\sqrt{\rho}}(x'_\times)\|_{d_\oplus,2}^2 & \text{if } g_i = \|\cdot - \cdot\|_{d_i,2}^2, \quad i = 1, \dots, N \\ \langle S_{\sqrt{\rho}}(x_\times), S_{\sqrt{\rho}}(x'_\times) \rangle_{d_\oplus} & \text{if } g_i = \langle \cdot, \cdot \rangle_{d_i}, \quad i = 1, \dots, N, \end{cases} \end{aligned}$$

where $S_{\sqrt{\rho}}(x_\times) := (\sqrt{\rho_1} x_1, \dots, \sqrt{\rho_N} x_N)$, $x_\times \in X_\times$. Thus,

$$(X_\times, m_\rho, \mu) \simeq \begin{cases} (\mathbb{R}^{d_\oplus}, \|\cdot - \cdot\|_{d_\oplus,2}^2, (S_{\sqrt{\rho}})_\# \mu) & \text{if } g_i = \|\cdot - \cdot\|_{d_i,2}^2, \quad i = 1, \dots, N \\ (\mathbb{R}^{d_\oplus}, \langle \cdot, \cdot \rangle_{d_\oplus}, (S_{\sqrt{\rho}})_\# \mu) & \text{if } g_i = \langle \cdot, \cdot \rangle_{d_i}, \quad i = 1, \dots, N. \end{cases}$$

For the above cases, our method provides us with embeddings without applying any distance-preserving embedding technique. However, it should be noted that these embeddings will naturally be high-dimensional. To reduce the dimensionality of the embedding, we may apply computationally inexpensive techniques such as the principle component analysis (PCA). In the special cases, where $\mu = (T_1, \dots, T_N)_\# \xi_1$ for isometries (or more generally linear functions) $T_i : X_1 \rightarrow X_i$, $i = 1, \dots, N$, the gm-space (X_\times, m_ρ, μ) is isomorphic to the (rescaled) graph of the linear function $(T_1, \dots, T_N) : X_1 \rightarrow \mathbb{R}^{d_\oplus}$, which is already a d_1 -dimensional subspace of \mathbb{R}^{d_\oplus} . Notably, this gives a further motivation for the linear Gromov–Monge problem [60, Def. 4.2.4], which naturally restricts the support of plans to lie on the graph of linear functions.

Surfaces. In the practical context, shapes are usually 2d surfaces that are embedded in the 3d Euclidean space. In mathematical terms this leads us to Riemannian manifolds. Let $M \subset \mathbb{R}^3$ be a smooth connected 2d manifold. The *Riemannian distance* on M is defined by

$$d_M(x, y) := \inf \left\{ \int_a^b \|\gamma'(t)\|_{3,2} dt : \gamma \in C^1([a, b], M), \gamma(a) = x, \gamma(b) = y \right\}.$$

Fortunately, Riemannian manifolds are isometric in the Riemannian sense if and only if they are isometric in the metric sense with respect to their Riemannian distance [37]. Let $M_i \subset \mathbb{R}^3$ be 2d Riemannian manifolds with Riemannian distances d_{M_i} and probability measures $\xi_i \in \mathcal{P}(M_i)$, $i = 1, \dots, N$. Consider the gm-spaces $\mathfrak{X}_i := (M_i, d_{M_i}^2, \xi_i)$. Using the fact that $\rho_i d_{M_i}^2(x_i, x'_i) = d_{\sqrt{\rho_i}M_i}^2(\sqrt{\rho_i}x_i, \sqrt{\rho_i}x'_i)$ and following similar arguments as in ii) of the previous paragraph, we can show that

$$(M_\times, m_\rho, \mu) \simeq (S_{\sqrt{\rho}}(M_\times), \tilde{d}_\rho, (S_{\sqrt{\rho}}) \# \mu),$$

where $M_\times := \times_{i=1}^N M_i$, $m_\rho := \sum_{i=1}^N \rho_i d_{M_i}^2$, and $\tilde{d}_\rho := \sum_{i=1}^N d_{\sqrt{\rho_i}M_i}^2$. The Cartesian product $S_{\sqrt{\rho}}(M_\times)$ is a $(2N)$ -dimensional Riemannian manifold embedded in \mathbb{R}^{3N} . Furthermore, \tilde{d}_ρ is the squared Riemannian distance on $S_{\sqrt{\rho}}(M_\times)$. Indeed, let $\gamma = (\gamma_1, \dots, \gamma_N)$ be an element of $C^1([a, b], S_{\sqrt{\rho}}(M_\times))$, then

$$\int_a^b \|\gamma'(t)\|_{3N,2}^2 dt = \int_a^b \sum_{i=1}^N \|\gamma'_i(t)\|_{3,2}^2 dt = \sum_{i=1}^N \int_a^b \|\gamma'_i(t)\|_{3,2}^2 dt.$$

Therefore, $\gamma \in C^1([a, b], S_{\sqrt{\rho}}(M_\times))$ realizes $d_{S_{\sqrt{\rho}}(M_\times)}$ if and only if all of its components γ_i realize $d_{\sqrt{\rho_i}M_i}$, $i = 1, \dots, N$ so that $\tilde{d}_\rho = d_{S_{\sqrt{\rho}}(M_\times)}$. Therefore, we may interpret the gm-space (M_\times, m_ρ, μ) as a $(2N)$ -dimensional Riemannian (product) manifold in \mathbb{R}^{3N} . If $\mu = (T_1, \dots, T_N) \# \xi_1$ for Riemannian isometries $T_i : M_1 \rightarrow M_i$, $i = 1, \dots, N$, we know that $\text{supp}(\mu) \subset S_{\sqrt{\rho}}(M_\times)$ admits a 2d isometric representative (e.g. M_1), however, in contrast to the Euclidean case, it is unclear if $\text{supp}(\mu)$ naturally lies on a lower-dimensional subspace of \mathbb{R}^{3N} .

7.3. Approximation of Pairwise Distances. In [10], the authors consider an approximation of pairwise GW distances of a set of spaces $\mathfrak{X}_i = \llbracket \mathfrak{X}_i \rrbracket = \llbracket (X_i, g_i, \xi_i) \rrbracket$, $i = 1, \dots, N$, by fixing a reference point $\mathfrak{Y} = \llbracket \mathfrak{Y} \rrbracket = \llbracket (Y, h, \nu) \rrbracket$, and proposing the *linear Gromov–Wasserstein distance*

$$\text{LGW}_{\mathfrak{Y}}(\mathfrak{X}_i, \mathfrak{X}_j) := \inf_{\substack{f_i \in \text{Log}_{\mathfrak{Y}}(\mathfrak{X}_i) \\ f_j \in \text{Log}_{\mathfrak{Y}}(\mathfrak{X}_j)}} d_{\mathfrak{X}_{\mathfrak{Y}}}(\mathfrak{f}_i, \mathfrak{f}_j) = \inf_{\substack{\mu_{i,j} \in \text{M}_{\mathfrak{Y}}(\pi_i, \pi_j) \\ \pi_i \in \Pi_o(\nu, \xi_i), \pi_j \in \Pi_o(\nu, \xi_j)}} F_{\text{GW}}^{\mathfrak{X}_i, \mathfrak{X}_j}(\mu_{i,j}),$$

where the second equality has been shown in the reference. The proposed distance follows the same idea as the so-called linear Wasserstein distance [64]: instead of directly computing the GW distance, the input spaces \mathfrak{X}_i , $i = 1, \dots, N$ are lifted into the tangent space of the a-priori fixed reference space \mathfrak{Y} via the logarithmic map, where subsequent distance computations are carried out. Because the logarithmic map is a set-valued function and thus may yield multiple tangents, and because the evaluated tangent distance $d_{\mathfrak{X}_{\mathfrak{Y}}}(\mathfrak{f}_i, \mathfrak{f}_j)$ is an upper bound to

$\text{GW}(\mathbb{X}_i, \mathbb{X}_j)$, the quantity is minimized with respect to all tangents in $\mathbb{L}\text{og}_{\mathbb{Y}}(\mathfrak{X}_i)$ and $\mathbb{L}\text{og}_{\mathbb{Y}}(\mathfrak{X}_j)$. Effectively, this results in minimizing with respect to all possible optimal GW plans from \mathbb{Y} to \mathbb{X}_i and \mathbb{X}_j . In practice, this minimization is intractable and is usually replaced by fixing one computed plan $\hat{\pi}_i$ per input \mathbb{X}_i , $i = 1, \dots, N$. After each iteration of [Algorithm 7.1](#), we obtain an approximation of $\text{LGW}_{\mathbb{Y}}(\mathfrak{X}_i, \mathfrak{X}_j)$ by evaluating $F_{\text{GW}}^{\mathbb{X}_i, \mathbb{X}_j}((P_{X_i \times X_j})_{\#}\mu)$, $i, j = 1, \dots, N$, where $\mu \in \mathbb{M}_{\mathbb{Y}}(\hat{\pi}_1, \dots, \hat{\pi}_N)$ is the measure obtained from the gluing-melting step. We explore this approximation in our numerical examples in further detail.

8. Numerical Experiments. We employ [Algorithm 7.1](#) together with our remarks of the previous section to interpolate and classify 3d shapes as well as for multi-graph matching on a protein network dataset. All experiments are run on an off-the-shelf MacBook Pro (Apple M1 chip, 8 GB RAM) and are implemented¹ in Python 3. We partly rely on the Python Optimal Transport (POT) toolbox [24], networkX [28] for handling graphs, Trimesh [19], as well as some publicized implementations of [65].

8.1. 3D Shape Interpolations. In the following, we use [Algorithm 7.1](#) paired with the considerations from [Section 7](#) to generate qualitative GW interpolations between multiple 3d surface meshes. We focus on two datasets, namely the mesh deformation dataset [58], which predominantly comprises animals in various poses. Furthermore, we consider the training subset of [14], which consists of 3d scans of humans in various poses. The meshes of the latter consist of 6890 nodes. Since some of the meshes from the mesh deformation dataset comprise up to 42k nodes, we use a quadric mesh simplification provided by the Trimesh package to reduce them to support sizes between 5000 and 6000.

From a surface mesh with nodes $V \subset \mathbb{R}^3$ and (triangular) faces $F \subset V^3$, we first extract a weighted graph $G = (V, E)$, where the edge set E is obtained by incorporating edges between any nodes which share a common face. The weight of the edge is given by the Euclidean distance between its respective nodes. From the graph (V, E) , we proceed to extract a gm-space $\mathbb{X} = (X, g, \xi)$ as follows: The node set serves as the support of \mathbb{X} , i.e. $X = V$, the gauge g is taken as the weighted Dijkstra distances between the individual nodes and ξ is the uniform distribution.

We utilize [Algorithm 7.1](#), to compute approximate barycenters between various choices of inputs $\mathbb{X}_i = (X_i, g_i, \xi_i)$, $i = 1, \dots, N$, for either $N = 2$ or $N = 4$. In all cases that follow, we set the initial guess to be one of the inputs, i.e. we initialize the algorithm with $\mathbb{Y} = \mathbb{X}_1$. As previously discussed, this reduces the computational complexity slightly. Moreover, to obtain the entire interpolation for $N = 2$ inputs, we only require one iteration of [Algorithm 7.1](#). More precisely, in this case, we merely compute an approximate optimal plan $\pi \in \Pi(\xi_1, \xi_2)$ via block-coordinate descent of the bi-convex relaxation. The barycenters then admit the form

$$(8.1) \quad \mathbb{Y}_{\rho} = (X_1 \times X_2, \rho_1 g_1 + \rho_2 g_2, \pi).$$

where $\rho_1 + \rho_2 = 1$. For $N = 4$, we restrict ourselves to 3 iterations of [Algorithm 7.1](#) which is indicated to be sufficient as we observed fast convergence in terms of the barycentric loss $\mathcal{F}_{\text{GWB}_{\rho}}^{\mathbb{X}_1, \dots, \mathbb{X}_N}$. As with $N = 2$, for the GW step we apply block-coordinate descent. For the gluing-melting step, we use the north-west-corner-rule, see [Section 7](#). For all but the first iteration,

¹The source code is publicly available at <https://github.com/robertbeinert/tangential-GW-barycenter>.

we initialize the block-coordinate descent in the GW step between $\mathbb{Y} = (X_\times, m_\rho, \mu)$ and \mathbb{X}_i with the plan $(P_{X_\times}, P_{X_i})_{\#}\mu \in \Pi(\mathbb{Y}, \mathbb{X}_i)$. Since the algorithm only requires the barycentric coordinates ρ for the mean gauge m_ρ in the final step and not in the main iteration to calculate the multi-marginal plan, we obtain approximate barycenters simultaneously for all $\rho \in \Delta_3$. The corresponding outputs admit the form

$$(8.2) \quad \mathbb{Y}_\rho = \left(\times_{i=1}^4 X_i, \sum_{i=1}^4 \rho_i g_i, \mu \right).$$

We remark that for these experiments, all obtained approximate GW transport plans were supported on the graph of a transport map, so that $|\text{supp}(\pi)| = |\text{supp}(\mu)| = 6890$. To construct appropriate surface meshes, we fix an index $i_0 \in \{1, \dots, N\}$ and incorporate a face between any three points $(x_1, \dots, x_N), (y_1, \dots, y_N), (z_1, \dots, z_N)$ in the support of the (approximate) barycenter whenever $(x_{i_0}, y_{i_0}, z_{i_0})$ is a face in the i_0 -th input. To plot the obtained meshes in 3d, we adopt the idea of [subsection 7.2](#) for the Euclidean case. For this, we replace the geodesic distances g_i in (8.1) and (8.2) with the squared Euclidean norm, i.e. we consider gm-spaces of the form

$$(\mathbb{R}^{3N}, \sum_{i=1}^N \rho_i \|\cdot - \cdot\|_{3,2}^2, \alpha) \simeq (\mathbb{R}^{3N}, \|\cdot - \cdot\|_{3N,2}^2, (S_{\sqrt{\rho}})_{\#}\alpha), \quad \alpha := \begin{cases} \pi & \text{for } N = 2, \\ \mu & \text{for } N = 4 \end{cases},$$

with $S_{\sqrt{\rho}}(x_\times) = (\sqrt{\rho_1}x_1, \dots, \sqrt{\rho_N}x_N)$. The support of $(S_{\sqrt{\rho}})_{\#}\alpha$ together with the previously constructed faces creates a $3N$ -dimensional surface mesh. Using a PCA, we compute an associated 3d affine subspace with the smallest projection error. Finally, we obtain 3d meshes by projecting onto the found subspace. Note that the replacement of the gauge together with the dimension reduction is merely a heuristic for plotting purposes.

For $N = 2$, [Figure 1](#) shows the obtained interpolations for $(\rho_1, \rho_2) = (5/6, 1/6), \dots, (1/6, 5/6)$ between various choices of meshes from both mentioned datasets. The colouring illustrates the transport between the inputs as well as between input and barycenter. We remark that the obtained interpolants do not follow any particular fixed alignment but have been rotated manually to align with the inputs for the purpose of comparison. In relation to the Euclidean diameters, the mean PCA errors, i.e. the mean distance of points before and after the PCA, are reasonably small. The results indicate that this feature is especially pronounced, if the GW distance between the associated inputs is small as well. Judging from a qualitative viewpoint, up to some small potential error, the obtained transport plans associated to $\mathbb{X}_1, \mathbb{X}_2$ of rows one and two are most likely global minimizers of $F_{\text{GW}}^{\mathbb{X}_1, \mathbb{X}_2}$. The optimality of the plan results in a very good shape interpolation between the inputs. In row three we see the results in the case where the obtained transport plan is most likely only a local minimum. As can be seen from the colours, the plan matches the left feet and right feet of the subjects correctly, but matches the left hand of the first subject with the right hand of the second and vice versa, which is evidently not a global minimum. This non-optimal matching is well reflected by the interpolation in which the legs seem to change places. Finally, the last row shows the results for a horse and a camel. It should be noted that the camel has, in contrast to the horse, a very short tail. Geodesically speaking, the inputs are thus very different. Indeed, as the colouring shows, the obtained transport plan matches the horse's tail to one of the camels legs

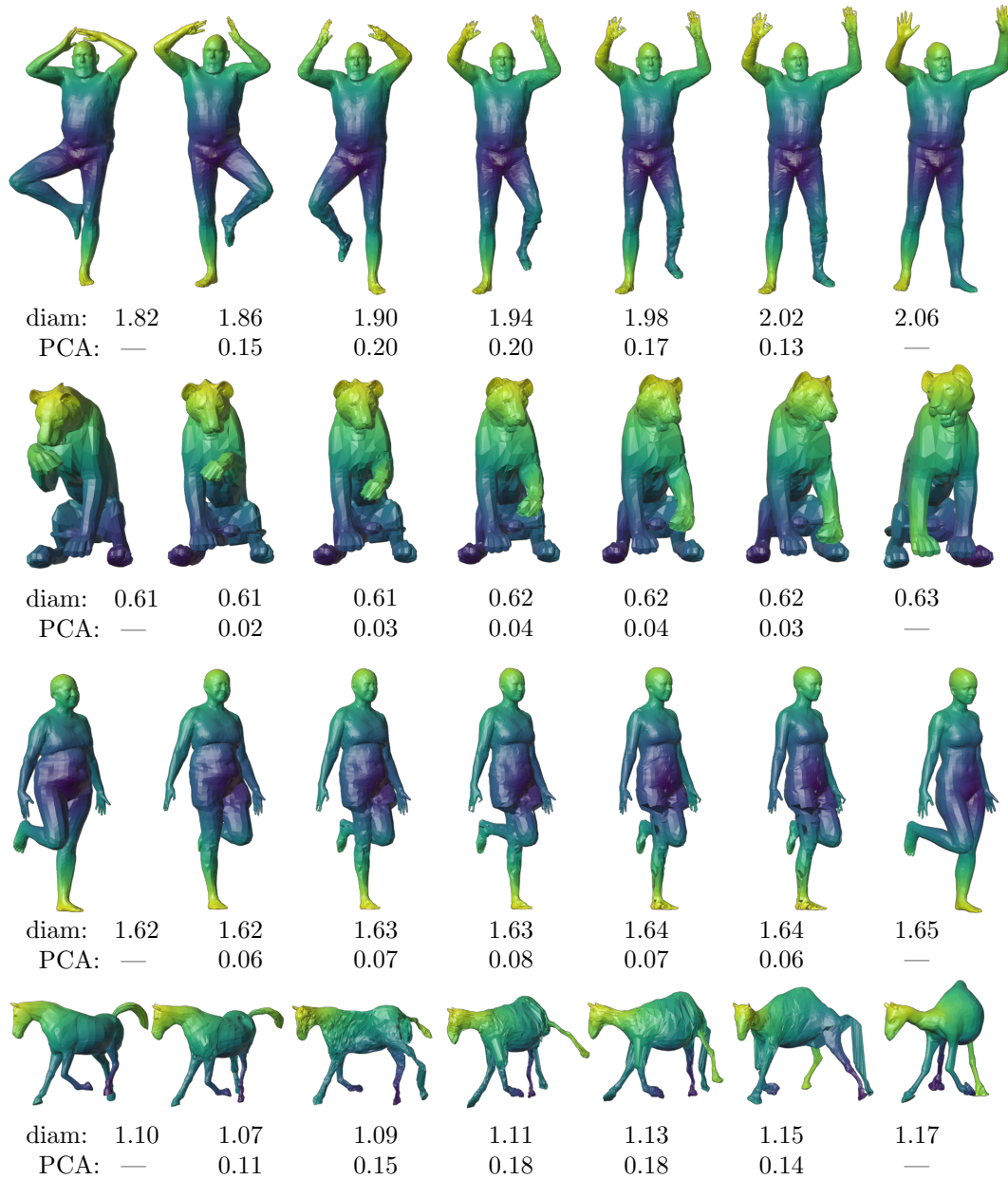


Figure 1: Gromov–Wasserstein interpolations $(\mathbb{Y}_\rho)_{\rho \in \Delta_1}$ between two 3d shapes for a total of four input pairs $(\mathbb{X}_1, \mathbb{X}_2)$. From left to right, each row shows $\mathbb{X}_1, \mathbb{Y}_{(5/6, 1/6)}, \mathbb{Y}_{(4/6, 2/6)}, \mathbb{Y}_{(3/6, 3/6)}, \mathbb{Y}_{(2/6, 4/6)}, \mathbb{Y}_{(1/6, 5/6)}, \mathbb{X}_2$. The colouring indicates the optimal GW plan between the inputs and interpolants. The Euclidean diameters (before applying the PCA) and PCA residuals are shown below each input/barycenter. The GW distances are (top to bottom): 0.07, 0.03, 0.06, 0.15.

and partially merges two of the horse’s legs to one. In the interpolation, the tail moves down the body to eventually become the leg of the camel.

The interpolation between $N = 4$ inputs are shown in [Figure 2](#). Different to the FAUST interpolations above, we picked four distinct subjects with distinct poses. Therefore, the challenge here is not only the interpolation between different body shapes but also between the poses. Judging from a qualitative viewpoint, our proposed method seems to overcome this suitably well. We want to emphasize again, that the entire interpolation is obtained by 3 iterations of [Algorithm 7.1](#). The quality of it suggests that the obtained melting μ seems to be at least near-optimal for $\text{MGW}_\rho(\mathbb{X}_1, \dots, \mathbb{X}_4)$ independently of $\rho \in \Delta_3$. Overall, the surfaces of the interpolants seem to be less smooth than those of the inputs. Here, the mean over all mean pca errors of all 21 barycenters is 0.11 and the mean Euclidean diameter of the 4 inputs is 1.92. which indicates that the PCA achieves a reasonable approximation.

8.2. Approximation of Pairwise Distances. According to [subsection 7.3](#), [Algorithm 7.1](#) provides us with an approximation of the pairwise linear GW distances of the inputs at a reference point. In this example, we show how these distances can be leveraged to classify shapes. As above, we focus on the training set of the FAUST dataset and the meshes from the deformation dataset. The former consists of 10 human subjects in 10 poses each, totaling to 100 meshes, whereas the latter consists in particular of the classes camel, cat, elephant, face, head, horse, lion, each of which is given in 10 or 11 poses. We reduce all meshes down to 500 nodes using the same quadric mesh decimation and extract the gm-spaces as in [subsection 8.1](#). We expect that identifying the classes from the deformation dataset with GW poses an easier task than identifying the subjects from the FAUST training set. This is due to the fact that the geometry between meshes from distinct classes of the deformation dataset varies much more than the geometry between distinct human subjects.

In the case of the deformation dataset, we extract $N = 73$ gm-spaces $\mathbb{X}_1, \dots, \mathbb{X}_N$. All gm-spaces are supported on 500 points and are endowed with their pairwise Dijkstra distances. As the meshes of distinct classes vary greatly in diameter, we rescale the gm-spaces so that the maximal Dijkstra distance of each is one. The classification task would be too simple otherwise. We proceed to compute all pairwise GW distances of the entire set with block-coordinate descent which takes approximately 43 minutes on our machine. As previously mentioned, the conditional gradient might only recover local minima. We use the following method to mitigate this problem. Since GW is a metric, we check if the triangle inequality holds for all inputs. Let $\pi_{i,j}$ be the obtained transport plan between \mathbb{X}_i and \mathbb{X}_j for all $i, j \in \{1, \dots, N\}$ and set $\text{GW}_{i,j} = F_{\text{GW}}^{\mathbb{X}_i, \mathbb{X}_j}(\pi_{i,j})$. Whenever there exists $k \in \{1, \dots, N\}$ so that $\text{GW}_{i,k} + \text{GW}_{k,j} < \text{GW}_{i,j}$ we know that $\pi_{i,j} \notin \Pi_o(\mathbb{X}_i, \mathbb{X}_j)$. In this case, we restart the block-coordinate descent for inputs $\mathbb{X}_i, \mathbb{X}_j$ with initial value $(P_{X_i \times X_j})_{\#} \gamma$, where $\gamma \in \Gamma_{\mathbb{X}_k}(\pi_{i,k}, \pi_{k,j})$ is the north-west-corner gluing between $\pi_{i,k}$ and $\pi_{k,j}$ along \mathbb{X}_k . The obtained pairwise distances are shown on the left-hand side of [Figure 3](#). As can be seen, the matrix of the pairwise distances readily identifies the classes. We verify this by a simple nearest-neighbour procedure. Here we run 10 000 iterations, in each of which we pick a random representative of each class. Afterwards, all shapes are classified using nearest neighbour classification with respect to the selected representatives. The confusion matrix is then estimated by considering the number of times a shape from class n has been classified as class m , for $n, m \in \{\text{camel, cat, elephant, face, head, horse, lion}\}$. The

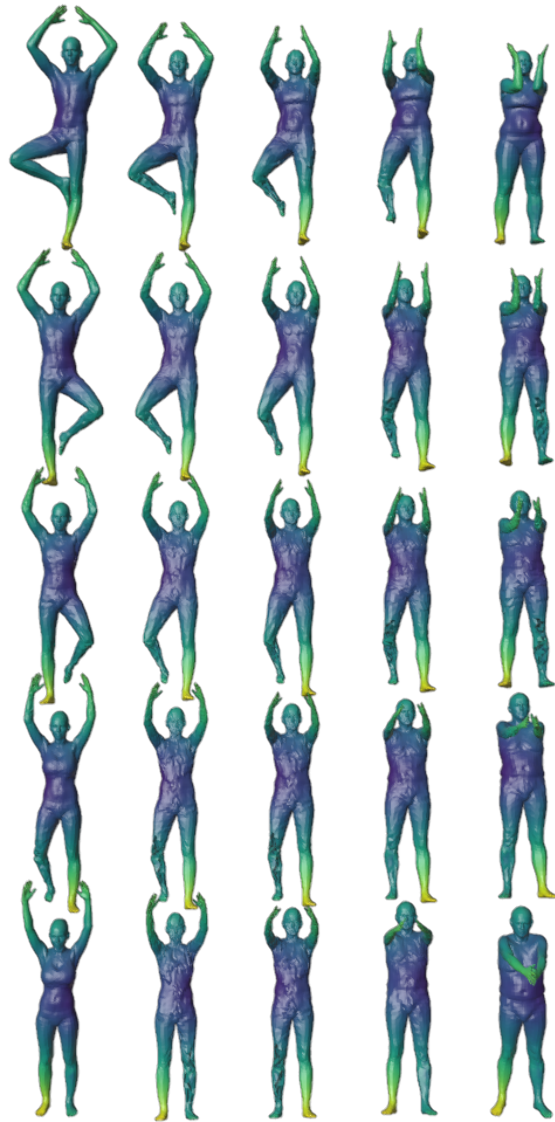


Figure 2: A GW interpolation $(\Upsilon_\rho)_{\rho \in \Delta_3}$ between four input shapes $\mathcal{X}_1, \mathcal{X}_2, \mathcal{X}_3, \mathcal{X}_4$ shown in the corners.

result is then normalized by the number of iterations and by the class-size. The resulting matrix is shown on the right-hand side of [Figure 3](#).

To quantify how well the linear approximation compares against the obtained GW distances, we run a 10-fold cross validation paired with a support vector machine to evaluate the potency for classification. More precisely, we split the set of N shapes into 10 subsets and perform 10 iterations in each of which 9 subsets are considered as a training set, whereas

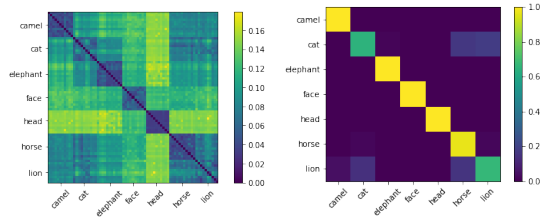


Figure 3: Pairwise GW distances (left) and confusion matrix (right) of the deformation dataset.

Table 1: Results of the 10-fold cross validation for the deformation dataset. The MRE and PCC are the means for the respective iterations over all iterations.

	Time (min)	Acc (%)	MRE	PCC
LGW ⁽¹⁾	1	83 ± 15	0.37 ± 0.14	0.73 ± 0.16
LGW ⁽²⁾	2	90 ± 13	0.25 ± 0.08	0.87 ± 0.10
LGW ⁽³⁾	3	95 ± 7	0.18 ± 0.03	0.94 ± 0.01
LGW ⁽⁴⁾	4	96 ± 6	0.17 ± 0.02	0.95 ± 0.02
LGW ⁽⁵⁾	5	97 ± 6	0.15 ± 0.01	0.96 ± 0.01
GW	43	97 ± 6	—	—

the remaining one is taken as a test set. In each iteration of the cross validation we do the following. Firstly, we run 5 iterations of *Algorithm 7.1*, initialized by setting \mathbb{Y} as a random element of the training set. In the gluing-melting step, we use the north-west corner rule. For $k = 1, \dots, 5$, let μ_k be the obtained melting after the k -th iteration. As elaborated in *subsection 7.3*, an approximation of the linear GW distance between $\mathbb{X}_i, \mathbb{X}_j$ at the reference $\mathbb{Y}^{(k-1)}$ is then obtained by setting

$$\text{LGW}_{i,j}^{(k)} := F_{\text{GW}}^{\mathbb{X}_i, \mathbb{X}_j}((P_{X_i \times X_j})_{\#} \mu_k).$$

In the following, for each $k = 1, \dots, 5$, we compare LGW^(k) with GW, within a larger machine-learning pipeline. To this end, we train two support vector machines with the kernels $\exp(-10 \text{GW}_{i,j})_{i,j}$ and $\exp(-10 \text{LGW}_{i,j}^{(k)})_{i,j}$ on the training set and evaluate on the test set. Additionally, we compute the mean relative error (MRE) and the Pearson correlation coefficient (PCC), of $(\text{GW}_{i,j})_{i,j}$ with respect to $(\text{LGW}_{i,j}^{(k)})_{i,j}$, $k = 1, \dots, 5$, where the mean is taken over all iterations of the cross validation. We remark that for the MRE, the 0 values of the matrices are not considered. The results are shown in *Table 1*. As we expected, GW is well suited for classifying the given shapes. The cross-validation shows that GW achieves an almost perfect classification. The linear approximation LGW^(k) achieves monotonous improvement in terms of accuracy, MRE and PCC. Furthermore, LGW⁽⁵⁾ achieves the same accuracy as the GW in terms of the cross validation process.

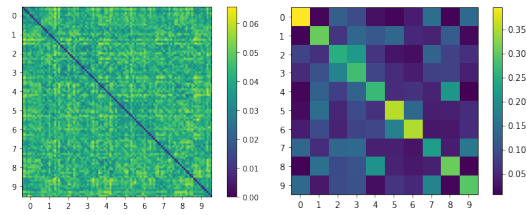


Figure 4: Pairwise GW distances (left) and confusion matrix (right) of the Faust dataset.

Table 2: Results of the 10-fold cross validation for the FAUST dataset. The MRE and PCC are the means for the respective iterations over all iterations.

	Time (min)	Acc (%)	MRE	PCC
LGW ⁽¹⁾	1	31 ± 8	0.19 ± 0.07	0.61 ± 0.16
LGW ⁽²⁾	2	41 ± 14	0.15 ± 0.01	0.64 ± 0.10
LGW ⁽³⁾	3	34 ± 13	0.15 ± 0.01	0.66 ± 0.07
LGW ⁽⁴⁾	4	44 ± 12	0.15 ± 0.02	0.63 ± 0.11
LGW ⁽⁵⁾	5	39 ± 16	0.15 ± 0.01	0.63 ± 0.10
GW	52	43 ± 13	—	—

We proceed analogously for $N = 100$ training meshes of the FAUST dataset. In this case, we have exactly 10 classes with 10 meshes per class. The pairwise distances together with the estimated confusion matrix are shown in Figure 3. The figure shows that, in terms of the GW distance, the differences between the classes are less pronounced. The results of the analogous 10-fold cross validation are presented in Table 2. As we expected, GW does not provide a very accurate classification of the dataset. In terms of the MRE and PCC, the linear approximation seems to converge faster than for the previous dataset. We postulate that this is due to the fact, that the dataset already consists of objects which lie all relatively close with respect to the GW distance. Thus the initial choice \mathbb{Y} (which is one of the input gm-spaces) already achieves a small barycenter loss. The accuracy based on the LGW seems to be less stable through the iterations but approximates the one based on GW suitably well.

8.3. Multi-graph matching of Protein networks. In this example, we explore our proposed methods potential for the task of multi-graph matching. We consider a dataset of $N = 6$ yeast networks which has been curated by Collins et al. [17]². The dataset has been used as a benchmark in e.g. [53, 61]. In addition, the dataset has been considered in [65] to gauge the effectiveness of a GW-based method to achieve a multi-graph matching. Although it seems that the authors utilize a GW barycenter for their proposed divide-and-conquer approach, the publicized source code reveals that the reported results are obtained by a greedy pairwise method. In the following, we want to show that our tangential barycenter may be leveraged

²The dataset can be downloaded from <https://www3.nd.edu/~cone/MAGNA++/>.

to obtain a viable multi-graph matching. We enumerate the yeast networks by $i = 1, \dots, 6$. The first network ($i = 1$) comes with 8323 high confidence protein-protein interactions (PPI). In addition to these high confidence PPIs, the other five networks ($i = 2, \dots, 6$) also exhibit $p\%$ (directed) low-confidence PPIs for $p \in \{5, 10, 15, 20, 25\}$. For each network their PPIs are stored as a matrix $M^{(i)} \in \{0, 1\}^{1004 \times 1004}$, where

$$M_{k,l}^{(i)} = \begin{cases} 0 & \text{protein } k \text{ interacts with protein } l. \\ 1 & \text{protein } k \text{ does not interact with protein } l. \end{cases}$$

Although PPIs are naturally symmetric, for reasons unaware to us, the stored matrices $M^{(i)}$ are not. Below we will resort to simple symmetrization to bypass this circumstance. Finally, on every network a probability measure ξ_i on the set of nodes is available, $i = 1, \dots, 6$. The dataset comes with the ground truth one-to-one correspondences between all networks.

We seek to apply our proposed method to achieve a multi-alignment of the given protein networks. To this end, let $X_1 = \dots = X_6 = \{1, \dots, 1004\}$, $g_i = \frac{1}{2}(M^{(i)} + (M^{(i)})^T)$ so that each network gives rise to a gm-space $\mathbb{X}_i := (X_i, g_i, \xi_i)$. We proceed to apply [Algorithm 7.1](#) four times on $\mathbb{X}_1, \dots, \mathbb{X}_n$, one time for each $n \in \{3, \dots, 6\}$ with initialization $\mathbb{Y} = \mathbb{X}_1$ and under the use of a proximal gradient descent to solve the inner GW computations. As we are interested in one-to-one matchings of the respective inputs the measures are constructed according to the maximum rule without replacement, see [Section 7](#). In this way, after each iteration of [Algorithm 7.1](#), we obtain a gm-space of the form $\mathbb{Y}_n := (\times_{i=1}^n X_i, \frac{1}{n} \sum_{i=1}^n g_i, \mu_n)$, where $|\text{supp } \mu_n| = 1004$. We iterate [Algorithm 7.1](#) until the barycentric loss $\mathcal{F}_{\text{GWB}_\rho}^{\mathbb{X}_1, \dots, \mathbb{X}_n}$ increases which results in 4,2,2,1 iterations for $n = 3, 4, 5, 6$, respectively. The multi-marginal matching between the n inputs is then encoded in the support points of the obtained multi-marginal plan μ_n , i.e.

$$(x_1, \dots, x_n) \in \times_{i=1}^n X_i \quad \text{are matched if} \quad (x_1, \dots, x_n) \in \text{supp}(\mu_n).$$

Inspired by [\[65\]](#), we employ the following two evaluation measures for node correctness

$$\begin{aligned} \text{NC@1} &:= \frac{|\{x \in \text{supp}(\mu_n) : \text{at least one pair } (x_k, x_l) \text{ for } k \neq l \text{ is matched correctly}\}|}{1004} \\ \text{NC@A} &:= \frac{|\{x \in \text{supp}(\mu_n) : \text{all } x_1, \dots, x_n \text{ are matched correctly}\}|}{1004}. \end{aligned}$$

The results as well as a comparison with those of [\[65\]](#) as they are reported in the reference are provided in [Table 3](#). It should be noted that the authors of [\[65\]](#) are using the non-symmetric matrices $M^{(i)}$ above as gauge functions for their methods. For a fair comparison against our method (GWTB), we repeat their experiments after replacing the adjacency matrices with the gauge functions g_i defined above which results are presented under GWL (sym). After symmetrization, the methods S-GWL and GWL yielded the same results. As we can see, our method performs (slightly) better than GWL (sym).

Table 3: Comparison of GWTB multi-graph matching with the one proposed in [65] for yeast network dataset.

Method	3 graphs		4 graphs		5 graphs		6 graphs	
	NC@1	NC@all	NC@1	NC@all	NC@1	NC@all	NC@1	NC@all
GWL	63.84	46.22	68.73	39.14	71.61	31.57	76.49	28.39
S-GWL	60.06	43.33	68.53	38.45	73.21	33.27	76.99	29.68
GWL (sym)	89.34	69.42	94.12	56.27	97.01	49.40	98.01	45.52
GWTB (ours)	93.32	69.92	96.81	61.35	97.21	52.09	98.90	45.52

Conclusions. In this paper, we show existence and characterize tangential GW barycenters, which gives rise to a novel method for approximating GW barycenters. We prove that the latter monotonously decreases the barycenter functional. We give numerical evidence that our proposed method can be used to obtain entire GW interpolations between multiple 3d shapes, for approximation of pairwise GW distances, as well as for multi-graph matching tasks. Another line of work, namely fused GW, aims at finding transport plans based on both the pairwise preservation of internal gauges as well as the preservation of labels in an additional label space. A generalization of our work to the fused case would require a careful study of the geometric structure of the labelled gm-spaces endowed with the fused GW distance which we leave as future work.

Funding. This work is supported in part by funds from the German Research Foundation (DFG) within the RTG 2433 DAEDALUS.

Appendix A. Proof of Theorem 5.1. The following is a slight generalization of the proof of [11, Thm 5.1]. First, notice that for for real numbers $a_1, \dots, a_N \in \mathbb{R}$, it holds

$$\sum_{i,j=1}^N \rho_i \rho_j |a_i - a_j|^2 = \sum_{i=1}^N \rho_i a_i^2 - \sum_{i,j=1}^N \rho_i \rho_j a_i a_j = \sum_{i=1}^N \rho_i |a_i| - \sum_{j=1}^N \rho_j |a_j|.$$

Thus

$$(A.1) \quad \min_{b \in \mathbb{R}} \sum_{i=1}^N \rho_i |a_i - b|^2 = \sum_{i=1}^N \rho_i |a_i| - \sum_{j=1}^N \rho_j |a_j|^2 = \sum_{i,j=1}^N \rho_i \rho_j |a_i - a_j|^2.$$

Hence, the integrand of $F_{\text{MGW}_\rho}^{\mathbb{X}_1, \dots, \mathbb{X}_N}(\pi)$, $\pi \in \Pi(\mathbb{X}_1, \dots, \mathbb{X}_N)$, becomes

$$\begin{aligned} \sum_{i,j=1}^N \rho_i \rho_j |g_i(x_i, x'_i) - g_j(x_j, x'_j)|^2 &= \sum_{i=1}^N \rho_i \left| g_i(x_i, x'_i) - \sum_{j=1}^N \rho_j g_j(x_j, x'_j) \right| \\ &= \sum_{i=1}^N \rho_i |g_i(x_i, x'_i) - m_\rho(x_\times, x'_\times)|. \end{aligned}$$

Now denote $\mathfrak{X}_i = [\mathbb{X}_i] = [(X_i, g_i, \xi_i)]$ and let $\mathfrak{Y} = [\mathbb{Y}] = [(Y, h, \nu)]$ be arbitrary. For $i = 1, \dots, N$ consider $\pi_i \in \Pi_o(\mathbb{X}_i, \mathbb{Y})$ and let $\gamma \in \Gamma_{\mathbb{Y}}(\pi_1, \dots, \pi_N)$. Pointwisely applying (A.1) with $a_i = g_i(x_i, x'_i)$ yields

$$\begin{aligned}
\mathcal{F}_{\text{GWB}_\rho}^{\mathbb{X}_1, \dots, \mathbb{X}_N}(\mathfrak{Y}) &= \sum_{i=1}^N \rho_i \text{GW}(\mathbb{X}_i, \mathbb{Y}) = \iint_{(X_\times \times Y)^2} \sum_{i=1}^N \rho_i |g_i - h| \, d\gamma \, d\gamma \\
&\geq \iint_{(X_\times \times Y)^2} \sum_{i,j=1}^N \rho_i \rho_j |g_i - g_j| \, d\gamma \, d\gamma \\
\text{(A.2)} \quad &= \iint_{X_\times^2} \sum_{i,j=1}^N \rho_i \rho_j |g_i - g_j| \, d(P_{X_\times})_{\#} \gamma \, d(P_{X_\times})_{\#} \gamma \geq \text{MGW}_\rho(\mathbb{X}_1, \dots, \mathbb{X}_N),
\end{aligned}$$

where the last estimate follows by $(P_{X_\times})_{\#} \gamma \in \Pi(\mathbb{X}_1, \dots, \mathbb{X}_N)$. We show that this lower bound is attained for $\hat{\mathfrak{Y}} = [\hat{\mathbb{Y}}] = [(X_\times, m_\rho, \hat{\pi})]$, where $\hat{\pi} \in \Pi_o(\mathbb{X}_1, \dots, \mathbb{X}_N)$ is arbitrary. Indeed, by defining $\hat{\pi}_i := (P_{X_i}, P_{X_\times})_{\#} \hat{\pi}$ and again using (A.1), it holds

$$\begin{aligned}
&\text{MGW}_\rho(\mathbb{X}_1, \dots, \mathbb{X}_N) \\
&= F_{\text{MGW}_\rho}^{\mathbb{X}_1, \dots, \mathbb{X}_N}(\hat{\pi}) = \iint_{X_\times^2} \sum_{i,j=1}^N \rho_i \rho_j |g_i - g_j| \, d\hat{\pi} \, d\hat{\pi} = \iint_{X_\times^2} \sum_{i=1}^N \rho_i |g_i - m_\rho| \, d\hat{\pi} \, d\hat{\pi} \\
&= \sum_{i=1}^N \rho_i \iint_{(X_i \times X_\times)^2} |g_i(x_i, x'_i) - m_\rho(y, y')| \, d\hat{\pi}_i(x_i, y) \, d\hat{\pi}_i(x'_i, y') \geq \sum_{i=1}^N \rho_i \text{GW}(\mathbb{X}_i, \hat{\mathbb{Y}}) \\
&= \mathcal{F}_{\text{GWB}_\rho}^{\mathbb{X}_1, \dots, \mathbb{X}_N}(\hat{\mathfrak{Y}}),
\end{aligned}$$

where the last estimate is due to $\hat{\pi}_i \in \Pi(\mathbb{X}_i, \hat{\mathbb{Y}})$. By the first part, $\hat{\mathfrak{Y}}$ is a solution to $\text{GWB}_\rho(\mathfrak{X}_1, \dots, \mathfrak{X}_N)$.

Now, let $\tilde{\mathfrak{Y}} = [\tilde{\mathbb{Y}}] = [(\tilde{Y}, \tilde{h}, \tilde{\nu})]$ be any minimizer of $\text{GWB}_\rho(\mathfrak{X}_1, \dots, \mathfrak{X}_N)$. We construct $\hat{\pi} \in \Pi_o(\mathbb{X}_1, \dots, \mathbb{X}_N)$ so that $\tilde{\mathfrak{Y}} = [(X_\times, m_\rho, \hat{\pi})]$. Let $\tilde{\gamma} \in \Gamma_{\tilde{\mathbb{Y}}}(\tilde{\pi}_1, \dots, \tilde{\pi}_N)$, where $\tilde{\pi}_i \in \Pi_o(\mathbb{X}_i, \tilde{\mathbb{Y}})$. By repeating the steps of (A.2) for $\mathfrak{Y} = \tilde{\mathfrak{Y}}$ and using that $\tilde{\mathfrak{Y}}$ is a solution of $\text{GWB}_\rho(\mathfrak{X}_1, \dots, \mathfrak{X}_N)$, we firstly obtain $\tilde{\pi} := (P_{X_\times})_{\#} \tilde{\gamma} \in \Pi_o^\rho(\mathbb{X}_1, \dots, \mathbb{X}_N)$ and secondly

$$\text{(A.3)} \quad \tilde{h}(\cdot_1, \cdot_3) = m_\rho(\cdot_2, \cdot_4) \quad (\tilde{\gamma} \otimes \tilde{\gamma})(\cdot_1, \cdot_2, \cdot_3, \cdot_4) - \text{a.s.},$$

where we also used (A.1) to receive the latter. Set $\hat{\mathbb{Y}} = (X_\times, m_\rho, \hat{\pi})$. By construction we have $\tilde{\gamma} \in \Pi(\tilde{\mathbb{Y}}, \hat{\mathbb{Y}})$. Using this together with (A.3), we obtain

$$\text{GW}(\tilde{\mathbb{Y}}, \hat{\mathbb{Y}})^2 \leq \iint_{(\tilde{Y} \times X_\times)^2} \underbrace{|\tilde{h} - m_\rho|^2}_{=0 \text{ a.e.}} \, d\tilde{\gamma} \, d\tilde{\gamma} = 0,$$

which concludes the proof.

Appendix B. Proof of Theorem 5.2.

Let $\rho \in \Delta_{N-1}$ be arbitrary and set $\hat{\pi} := (T_1, \dots, T_N)_{\#}\xi_1$. Note that $\xi_1 = (T_1)_{\#}\xi_1$. Therefore, without loss of generality, we set $T_1 = \text{Id}_{\mathbb{R}^{d_1}}$. In the following, we rely on [21, Prop 4.1] which states

$$(P_{X_1 \times X_i})_{\#}\hat{\pi} = (\text{Id}_{\mathbb{R}^{d_1}}, T_i)_{\#}\xi_1 \in \Pi_o(\mathbb{X}_1, \mathbb{X}_i).$$

Consequently, $\hat{\pi} \in \Pi(\mathbb{X}_1, \dots, \mathbb{X}_N)$. Next, we show $(P_{X_i \times X_j})_{\#}\hat{\pi} \in \Pi_o(\mathbb{X}_i, \mathbb{X}_j)$ for all $i, j = 1, \dots, N$, which yields $\hat{\pi} \in \Pi_o^0(\mathbb{X}_1, \dots, \mathbb{X}_N)$ due to

$$\begin{aligned} \frac{1}{2} \sum_{i,j=1}^N \rho_i \rho_j \text{GW}(\mathbb{X}_i, \mathbb{X}_j) &\leq \text{MGW}_{\rho}(\mathbb{X}_1, \dots, \mathbb{X}_N) \leq F_{\text{MGW}_{\rho}}^{\mathbb{X}_1, \dots, \mathbb{X}_N}(\hat{\pi}) \\ &= \frac{1}{2} \sum_{i,j=1}^N \rho_i \rho_j F_{\text{GW}}^{\mathbb{X}_i, \mathbb{X}_j}((P_{X_i \times X_j})_{\#}\hat{\pi}) = \frac{1}{2} \sum_{i,j=1}^N \rho_i \rho_j \text{GW}(\mathbb{X}_i, \mathbb{X}_j). \end{aligned}$$

Let $i \leq j$ and set

$$S : \mathbb{R}^{d_i} \rightarrow \mathbb{R}^{d_j}, \quad S(x) = P_j B P_i^{\text{T}} x, \quad B = \left(\tilde{I}_{d_j} \tilde{I}_{d_i}^{(d_j)} D_j^{1/2} \left(D_i^{(d_j)} \right)^{-1/2} \mid 0_{d_j, d_i-d_j} \right) \in \mathbb{R}^{d_j \times d_i}.$$

We have

$$\begin{aligned} B A_i &= \left(\tilde{I}_{d_j} \tilde{I}_{d_i}^{(d_j)} D_j^{1/2} \left(D_i^{(d_j)} \right)^{-1/2} \mid 0_{d_j, d_i-d_j} \right) \left(\tilde{I}_{d_i} D_i^{1/2} \left(D_1^{(d_i)} \right)^{-1/2} \mid 0_{d_i, d_1-d_i} \right) \\ &= \left(\tilde{I}_{d_j} \tilde{I}_{d_i}^{(d_j)} D_j^{1/2} \left(D_i^{(d_j)} \right)^{-1/2} \tilde{I}_{d_i}^{(d_j)} \left(D_i^{1/2} \right)^{(d_j)} \left(\left(D_1^{(d_i)} \right)^{-1/2} \right)^{(d_j)} \mid 0_{d_j, d_1-d_j} \right). \end{aligned}$$

As all matrices in the left block are diagonal, they commute. Applying this together with $(D_i^{1/2})^{(d_j)} = (D_i^{(d_j)})^{1/2}$ and $((D_1^{(d_i)})^{-1/2})^{(d_j)} = ((D_1^{(d_j)})^{-1/2})$, we obtain

$$B A_i = \left(\tilde{I}_{d_j} D_j^{1/2} \left(D_1^{(d_j)} \right)^{-1/2} \mid 0_{d_j, d_1-d_j} \right) = A_j.$$

Hence, $S \circ T_i = P_j B P_i^{\text{T}} P_i A_i P_1^{\text{T}} = P_j B A_i P_1^{\text{T}} = P_j A_j P_1^{\text{T}} = T_j$. This shows the first part due to

$$(P_{X_i \times X_j})_{\#}\hat{\pi} = (T_i, T_j)_{\#}\xi_1 = (T_i, S T_i)_{\#}\xi_1 = (\text{Id}_{\mathbb{R}^{d_i}}, S)_{\#}\xi_i \in \Pi_o(\mathbb{X}_i, \mathbb{X}_j),$$

where the latter inclusion is again provided by [21, Prop. 4.1].

We turn our attention to the barycenter statement. As $\text{GWB}_{\rho}(\mathbb{X}_1, \dots, \mathbb{X}_N)$ is independent of orthogonal transformations of the inputs, we assume without loss of generality that $\Sigma_i = D_i$ which gives $T_i = A_i$. Let $d_{\oplus} := \sum_{i=1}^N d_i$. Combining the first part with Theorem 5.1 yields that the gm-space

$$(\mathbb{R}^{d_{\oplus}}, \sum_{i=1}^N \rho_i \langle \cdot, \cdot \rangle_{d_i}, \hat{\pi}) = (\mathbb{R}^{d_{\oplus}}, \sum_{i=1}^N \rho_i \langle \cdot, \cdot \rangle_{d_i}, (A_1, \dots, A_N)_{\#}\xi_1),$$

is a solution of $\text{GWB}_{\rho}(\mathbb{X}_1, \dots, \mathbb{X}_N)$ for all $\rho \in \Delta_{N-1}$. For $x, x' \in \mathbb{R}^{d_1}$, it holds

$$\begin{aligned} \sum_{i=1}^N \rho_i \langle A_i x, A_i x' \rangle_{d_i} &= \sum_{i=1}^N \rho_i x^{\text{T}} A_i^{\text{T}} A_i x' = x^{\text{T}} \underbrace{\sum_{i=1}^N \rho_i A_i^{\text{T}} A_i}_{=: M \text{ (diagonal)}} x' = \langle M^{1/2} x, M^{1/2} x' \rangle_{d_1}. \end{aligned}$$

Thus, we obtain

$$\begin{aligned} (\mathbb{R}^{d_\oplus}, \sum_{i=1}^N \rho_i \langle \cdot, \cdot \rangle_{d_i}, \hat{\pi}) &\simeq (\mathbb{R}^{d_1}, \sum_{i=1}^N \rho_i \langle A_i \cdot, A_i \cdot \rangle_{d_i}, \xi_1) \\ &\simeq (\mathbb{R}^{d_1}, \langle M^{1/2} \cdot, M^{1/2} \cdot \rangle_{d_1}, \xi_1) \\ &\simeq (\mathbb{R}^{d_1}, \langle \cdot, \cdot \rangle_{d_1}, (M^{1/2})_{\#} \xi_1). \end{aligned}$$

Finally, $(M^{1/2})_{\#} \xi_1$ is a centered Gaussian distribution on \mathbb{R}^{d_1} , whose covariance matrix is given by

$$M^{1/2} \Sigma_1 (M^{1/2})^T = M D_1 = \sum_{i=1}^N \rho_i A_i^T A_i D_1 = \sum_{i=1}^N \rho_i \begin{pmatrix} D_i (D_1^{(d_i)})^{-1} & 0 \\ 0 & 0 \end{pmatrix} D_1 = \sum_{i=1}^N \rho_i \begin{pmatrix} D_i & 0 \\ 0 & 0 \end{pmatrix},$$

which concludes the proof.

REFERENCES

- [1] M. Agueh and G. Carlier. Barycenters in the Wasserstein space. *SIAM J. Math. Anal.*, 43(2):904–924, 2011.
- [2] F. Altekrieger, J. Hertrich, and G. Steidl. Neural Wasserstein gradient flows for maximum mean discrepancies with Riesz kernels. *arXiv:2301.11624*, 2023.
- [3] P. C. Álvarez Esteban, E. del Barrio, J. A. Cuesta-Albertos, and C. Matrán. A fixed-point approach to barycenters in Wasserstein space. *J. Math. Anal. Appl.*, 441(2):744–762, 2016.
- [4] D. Alvarez-Melis and T. S. Jaakkola. Gromov–Wasserstein alignment of word embedding spaces. *arXiv:1809.00013*, 2018.
- [5] L. Ambrosio, E. Brué, and D. Semola. *Lectures on Optimal Transport*. Number 130 in Unitext. Springer, Cham, 2021.
- [6] L. Ambrosio, N. Gigli, and G. Savaré. *Gradient Flows in Metric Spaces and in the Space of Probability Measures*. Birkhäuser, Basel, 2005.
- [7] M. Arbel, A. Korba, A. Salim, and A. Gretton. Maximum mean discrepancy gradient flow. In H. Wallach, H. Larochelle, A. Beygelzimer, F. d Alché-Buc, E. Fox, and R. Garnett, editors, *Advances in Neural Information Processing Systems*, volume 32, pages 1–11, New York, USA, 2019. Curran Associates Inc.
- [8] M. Arjovsky, S. Chintala, and L. Bottou. Wasserstein generative adversarial networks. In *Proc. of Machine Learning*, volume 70, pages 214–223. PMLR, 2017.
- [9] F. Beier. Gromov–Wasserstein transfer operators. In *International Conference on Scale Space and Variational Methods in Computer Vision*, pages 614–626. Springer, 2023.
- [10] F. Beier, R. Beinert, and G. Steidl. On a linear Gromov–Wasserstein distance. *IEEE Trans. Image Process.*, 31:7292–7305, 2022.
- [11] F. Beier, R. Beinert, and G. Steidl. Multi-marginal Gromov–Wasserstein transport and barycentres. *Inf. Inference*, 12(4):2753–2781, 10 2023.
- [12] F. Beier, J. von Lindheim, S. Neumayer, and G. Steidl. Unbalanced multi-marginal optimal transport. *J. Math. Imaging Vis.*, 65(3):394–413, 2023.
- [13] R. Beinert, C. Heiss, and G. Steidl. On assignment problems related to Gromov–Wasserstein distances on the real line. *SIAM J. Imaging Sci.*, 16(2):1028–1032, 2023.
- [14] F. Bogo, J. Romero, M. Loper, and M. J. Black. FAUST: Dataset and evaluation for 3D mesh registration. In *Proceedings IEEE Conf. on Computer Vision and Pattern Recognition (CVPR)*, Piscataway, NJ, USA, June 2014. IEEE.
- [15] G. Carlier and I. Ekeland. Matching for teams. *Econ. Theory*, 42:397–418, 02 2010.
- [16] S. Chowdhury and T. Needham. Gromov–Wasserstein averaging in a Riemannian framework. In *Proceedings of the IEEE/CVF Conference on Computer Vision and Pattern Recognition Workshops*, pages 842–843, 2020.

- [17] S. R. Collins, P. Kemmeren, X.-C. Zhao, J. F. Greenblatt, F. Spencer, F. C. Holstege, J. S. Weissman, and N. J. Krogan. Toward a comprehensive atlas of the physical interactome of *saccharomyces cerevisiae*. *Mol. Cell. Proteom.*, 6(3):439–450, 2007.
- [18] M. Cuturi. Sinkhorn distances: lightspeed computation of optimal transport. In *Advances in Neural Information Processing Systems 26*, pages 2292–2300. Curran Associates, Inc., 2013.
- [19] Dawson-Haggerty et al. Trimesh, 2019. <https://trimesh.org/>, version 3.2.0.
- [20] J. Delon and A. Desolneux. A Wasserstein-type distance in the space of Gaussian mixture models. *SIAM J. Imaging Sci.*, 13(2):936–970, 2020.
- [21] J. Delon, A. Desolneux, and A. Salmona. Gromov–Wasserstein distances between Gaussian distributions. *J. Appl. Probab.*, 59(4):1178–1198, 2022.
- [22] M. Ehler, M. Gräf, S. Neumayer, and G. Steidl. Curve based approximation of measures on manifolds by discrepancy minimization. *Found. Comp. Math.*, 21(6):1595–1642, 2021.
- [23] F. Elvander, I. Haasler, A. Jakobsson, and J. Karlsson. Multi-marginal optimal transport using partial information with applications in robust localization and sensor fusion. *Signal Process.*, 171:107474, 2020.
- [24] R. Flamary, N. Courty, A. Gramfort, M. Z. Alaya, A. Boisbunon, S. Chambon, L. Chapel, A. Corenflos, K. Fatras, N. Fournier, L. Gautheron, N. T. Gayraud, H. Janati, A. Rakotomamonjy, I. Redko, A. Rolet, A. Schutz, V. Seguy, D. J. Sutherland, R. Tavenard, A. Tong, and T. Vayer. POT: Python optimal transport. *J. Mach. Learn. Res.*, 22(78):1–8, 2021.
- [25] A. Forrow, J.-C. Hütter, M. Nitzan, P. Rigollet, G. Schiebinger, and J. Weed. Statistical optimal transport via factored couplings. In *The 22nd International Conference on Artificial Intelligence and Statistics*, pages 2454–2465. PMLR, 2019.
- [26] G. Friesecke and M. Penka. The GenCol algorithm for high-dimensional optimal transport: general formulation and application to barycenters and Wasserstein splines. *SIAM J. Math. Data Sci.*, 5(4):899–919, 2023.
- [27] C. Frogner, C. Zhang, H. Mobahi, M. Araya, and T. A. Poggio. Learning with a Wasserstein loss. In *Advances in Neural Information Processing Systems 28*, pages 2053–2061. Curran Associates, Inc., 2015.
- [28] A. A. Hagberg, D. A. Schult, and P. J. Swart. Exploring network structure, dynamics, and function using NetworkX. In G. Varoquaux, T. Vaught, and J. Millman, editors, *Proceedings of the 7th Python in Science Conference*, pages 11–15, 2008.
- [29] P. Hagemann, J. Hertrich, F. Altekürger, R. Beinert, J. Chemseddine, and G. Steidl. Posterior sampling based on gradient flows of the MMD with negative distance kernel. *arXiv:2310.03054*, 2024.
- [30] J. Hertrich, R. Beinert, M. Gräf, and G. Steidl. Wasserstein gradient flows of the discrepancy with distance kernel on the line. In *International Conference on Scale Space and Variational Methods in Computer Vision*, pages 431–443. Springer, 2023.
- [31] J. Hertrich, M. Gräf, R. Beinert, and G. Steidl. Wasserstein steepest descent flows of discrepancies with Riesz kernels. *J. Math. Anal. Appl.*, 531(1):127829, 2024.
- [32] R. Jordan, D. Kinderlehrer, and F. Otto. The variational formulation of the Fokker–Planck equation. *SIAM J. Math. Anal.*, 29(1):1–17, 1998.
- [33] O. Junge, D. Matthes, and B. Schmitzer. Entropic transfer operators. *arXiv:2204.04901*, 2022.
- [34] P. Koltai, J. von Lindheim, S. Neumayer, and G. Steidl. Transfer operators from optimal transport plans for coherent set detection. *Phys. D*, 426:132980, 2021.
- [35] M. Kusner, Y. Sun, N. Kolkin, and K. Weinberger. From word embeddings to document distances. In *Proc. of Machine Learning Research*, volume 37, pages 957–966. PMLR, 2015.
- [36] K. Le, D. Q. Le, H. Nguyen, D. Do, T. Pham, and N. Ho. Entropic Gromov-Wasserstein between Gaussian distributions. In K. Chaudhuri, S. Jegelka, L. Song, C. Szepesvari, G. Niu, and S. Sabato, editors, *Proceedings of the 39th International Conference on Machine Learning*, volume 162 of *Proceedings of Machine Learning Research*, pages 12164–12203. PMLR, 17–23 Jul 2022.
- [37] J. M. Lee. *Introduction to Riemannian manifolds*, volume 2. Springer, 2018.
- [38] F. Méoli. Gromov–Wasserstein distances and the metric approach to object matching. *Found. Comput. Math.*, 11(4):417–487, 2011.
- [39] C. Moosmüller and A. Cloninger. Linear optimal transport embedding: provable Wasserstein classification for certain rigid transformations and perturbations. *Inf. Inference*, 12(1):363–389, 2023.

- [40] S. Neumayer, V. Stein, and G. Steidl. Wasserstein gradient flows for Moreau envelopes of f -divergences in reproducing kernel Hilbert spaces. *arXiv:2402.04613*, 2024.
- [41] D. H. Nguyen and K. Tsuda. On a linear fused Gromov–Wasserstein distance for graph structured data. *Pattern Recognit.*, 138:109351, 2023.
- [42] F. Otto. The geometry of dissipative evolution equations: the porous medium equation. *Comm. Partial Differential Equations*, 26:101–174, 2001.
- [43] B. Pass. Multi-marginal optimal transport: theory and applications. *ESAIM Math. Model. Numer. Anal.*, 49(6):1771–1790, 2015.
- [44] G. A. Pavliotis. *Stochastic Processes and Applications: Diffusion Processes, the Fokker–Planck and Langevin Equations*. Number 60 in Texts in Applied Mathematics. Springer, New York, 2014.
- [45] X. Pennec. Intrinsic statistics on Riemannian manifolds: basic tools for geometric measurements. *J. Math. Imaging Vis.*, 25(1):127–154, 2006.
- [46] G. Peyré and M. Cuturi. Computational optimal transport: with applications to data science. *Found. Trends Mach. Learn.*, 11(5-6):355–607, 2019.
- [47] G. Peyré, M. Cuturi, and J. Solomon. Gromov-Wasserstein averaging of kernel and distance matrices. In *International Conference on Machine Learning*, pages 2664–2672, 2016.
- [48] M. Quellmalz, R. Beinert, and G. Steidl. Sliced optimal transport on the sphere. *Inverse Probl.*, 39(10):105005, 2023.
- [49] M. Quellmalz, L. Buecher, and G. Steidl. Parallely sliced optimal transport on spheres and on the rotation group. *arXiv:2401.16896*, 2024.
- [50] J. Rabin, G. Peyré, J. Delon, and M. Bernot. Wasserstein barycenter and its application to texture mixing. In *International Conference on Scale Space and Variational Methods in Computer Vision*, pages 435–446. Springer, 2011.
- [51] M. Ryner, J. Kronqvist, and J. Karlsson. Globally solving the Gromov-Wasserstein problem for point clouds in low dimensional Euclidean spaces. In A. Oh, T. Neumann, A. Globerson, K. Saenko, M. Hardt, and S. Levine, editors, *Advances in Neural Information Processing Systems*, volume 36, pages 7930–7946. Curran Associates, Inc., 2023.
- [52] F. Santambrogio. {Euclidean, metric, and Wasserstein} gradient flows: an overview. *Bull. Math. Sci.*, 7(1):87–154, 2017.
- [53] V. Saraph and T. Milenković. MAGNA: maximizing accuracy in global network alignment. *Bioinform.*, 30(20):2931–2940, 07 2014.
- [54] M. Scetbon, M. Cuturi, and G. Peyré. Low-rank Sinkhorn factorization. In *International Conference on Machine Learning*, pages 9344–9354. PMLR, 2021.
- [55] M. Scetbon, G. Peyré, and M. Cuturi. Linear-time Gromov Wasserstein distances using low rank couplings and costs. In *International Conference on Machine Learning*, pages 19347–19365. PMLR, 2022.
- [56] K.-T. Sturm. On the geometry of metric measure spaces. *Acta Math.*, 196(1):65–131, 2006.
- [57] K.-T. Sturm. The space of spaces: curvature bounds and gradient flows on the space of metric measure spaces. *arXiv:1208.0434*, 2020.
- [58] R. W. Sumner and J. Popovic. Mesh data from deformation transfer for triangle meshes. <http://people.csail.mit.edu/sumner/research/deftransfer/data.html>.
- [59] V. Titouan, R. Flamary, N. Courty, R. Tavenard, and L. Chapel. Sliced Gromov-Wasserstein. In H. Wאלlach, H. Larochelle, A. Beygelzimer, F. Alché-Buc, E. Fox, and R. Garnett, editors, *Advances in Neural Information Processing Systems*, volume 32. Curran Associates, Inc., 2019.
- [60] T. Vayer. A contribution to optimal transport on incomparable spaces. *PhD Thesis, Université Bretagne*, 2020.
- [61] V. Vijayan, V. Saraph, and T. Milenković. Magna++: maximizing accuracy in global network alignment via both node and edge conservation. *Bioinform.*, 31(14):2409–2411, 03 2015.
- [62] C. Villani. *Optimal Transport: Old and New*, volume 338. Springer, 2008.
- [63] J. von Lindheim. Simple approximative algorithms for free-support Wasserstein barycenters. *Comput. Optim. Appl.*, 85(1):213–246, 2023.
- [64] W. Wang, D. Slepčev, S. Basu, J. A. Ozolek, and G. K. Rohde. A linear optimal transportation framework for quantifying and visualizing variations in sets of images. *Int. J. Comput. Vis.*, 101(2):254–269, 2013.
- [65] H. Xu, D. Luo, and L. Carin. Scalable Gromov–Wasserstein learning for graph partitioning and matching. *Advances in neural information processing systems*, 32, 2019.

-
- [66] L. Zhu, Y. Yang, S. Haker, and A. Tannenbaum. An image morphing technique based on optimal mass preserving mapping. *IEEE Trans. Image Process.*, 16:1481–95, 2007.